




Deep phenotyping of miRNAs in exercise-induced cardiac hypertrophy and fibrosis

MUKADDES PALA^{1*}, SENAY GORUCU YILMAZ², MEHMET ALTAN³,
OSMAN FUAT SONMEZ³, SENSU DINCER⁴, MURAT MENGI⁵,
AYDIN KARABULUT⁶, FAHRIYE SECIL TECELLIOGLU⁷, FAHRI AKBAS⁸,
MUSTAFA YILDIZ⁹, MELTEM KUMAS KULUALP¹⁰, MUKADDES ESREFOGLU¹¹
and GOKHAN METIN⁴

¹Department of Physiology, Medical Faculty, Malatya Turgut Ozal University, Malatya, Turkey

²Department of Nutrition and Dietetics, Health Science Faculty, Gaziantep University, Gaziantep, Turkey

³Department of Physiology, Cerrahpasa Medical Faculty, Istanbul University, Istanbul, Turkey

⁴Department of Sports Medicine, Istanbul Medical Faculty, Istanbul University, Istanbul, Turkey

⁵Department of Physiology, Medical Faculty, Namik Kemal University, Tekirdag, Turkey

⁶Department of Immunology, Hamidiye Health Science Institute, Health Science University, Istanbul, Turkey

⁷Department of Pathology, Medical Faculty, Malatya Turgut Ozal University, Malatya, Turkey

⁸Department of Medical Biology, Medical Faculty, Bezmialem Vakif University, Istanbul, Turkey

⁹Institute of Cardiology, Istanbul University, Istanbul, Turkey

¹⁰Department of Histology and Embryology, Veterinary Faculty, Dokuz Eylul University, Izmir, Turkey

¹¹Department of Histology and Embryology, Medical Faculty, Bezmialem Vakif University, Istanbul, Turkey

*Corresponding author (Email, mukaddes.pala@ozal.edu.tr)

MS received 6 July 2021; accepted 6 March 2023

Cardiac hypertrophy (CH) is an adaptational enlargement of the myocardium, in exposure to altered stress conditions or in case of injury which can lead to heart failure and death. MicroRNAs (miRNAs) are non-coding RNAs that play a significant role in modulating gene expression. Here, we aimed to identify new miRNAs effective in an experimental CH model and to find an epigenetic biomarker that could demonstrate therapeutic targets responsible for the pathology of heart tissue and serum. In this study, Sprague–Dawley male rats were divided into the training group (TG, $n=9$) and the control group (CG, $n=6$). Systolic and diastolic dimensions of the left ventricle and myocardial wall thickness were measured by echocardiography to assess CH. After the exercise program of the rats, miRNA expression measurements and histological analyses were performed. The 25,000 genes in the rat genome were searched using microarray analysis. A total of 128 miRNAs were selected according to the fold change rates, and nine miRNAs were validated for expression analysis. The terminal deoxynucleotidyl transferase dUTP nick (TUNEL) method was used to detect apoptotic cells. Cell proliferation was evaluated by the proliferative cell nuclear antigen (PCNA) method. Necrosis, bleeding, and intercellular edema were detected in TG. The mean histopathological score was higher in TG ($p=0.03$). There were rarely positive cells for apoptosis of both groups in cardiomyocytes. In the receiver characteristic curve analysis (ROC), the heart tissue *rno-miR-290* had an area under the curve (AUC) of 0.920 with 100% sensitivity and 89.90% specificity ($p=0.045$), *rno-miR-194-5p* had AUC of 0.940 with 83.33% sensitivity and 100% specificity ($p=0.003$), and the serum *rno-miR-132-3p* AUC was 0.880 with 66.67%

sensitivity and 100% specificity ($p=0.004$) in TG. miR-194-5p was used as a therapeutic target for remodeling the cardiac process. While miR-290 contributes to CH as a negative regulator, miR-132 in serum is effective in the pathological and physiological cardiac remodeling process and is a candidate biomarker.

Keywords. Biomarker; cardiac hypertrophy; circulating miRNAs; gene expression; miRNA expression; swimming training

1. Introduction

Cardiac hypertrophy (CH) is an adaptive enlargement of the myocardium against different stress conditions or injuries (Stansfield *et al.* 2014). Occasionally, it is a pathological feature seen in various diseases such as hypertension, ischemic myocardial damage, diabetic cardiomyopathy, heart diseases associated with aortic stenosis, and valvular dysfunction (Oktay *et al.* 2020). The pathological CH process can cause ventricular dilatation, arrhythmia, fibrotic diseases, heart failure, and even sudden death (Cunningham *et al.* 2019). Apart from the pathological conditions, regular endurance-type exercise programs increase aerobic capacity which may lead to CH in a physiological adaptive process (Hughes *et al.* 2018). Fibrosis is a pathological feature common for various types of heart disease. The cellular basis of fibrosis is the abnormal accumulation of collagen and extracellular matrix (ECM) proteins that impair ventricular function and cause a tendency to arrhythmia in the heart (van Rooij and Olson 2009). Cardiac fibrosis (CF) results from increased proliferation of fibroblasts and accumulation of ECM. The development of fibrosis causes cardiac dysfunction and heart failure (Wijnen *et al.* 2013).

Exercise is a physical activity that creates natural stress conditions in an organism and increases performance through various adaptation mechanisms depending on the systematic repetition of movement processes (Evangelista *et al.* 2003). Carefully planned programs are needed for exercise-related adaptations to develop. These programs should include factors such as type, intensity, duration, frequency of exercise, and rest intervals. There are differences in the adaptations that occur according to the type of exercise chosen. In aerobic exercise (AE), large muscle groups that cause an increase in heart rate and acceleration in respiration are used (Evangelista *et al.* 2003). During exercise, there is an increase in both the heart rate and the amount of oxygen consumed (VO_2 max) due to increased workload. When the intensity of the exercise increases, cardiovascular loading and muscle performance, which are adaptations specific to the aerobic

system, are observed, while the increase in VO_2 max is lower when the intensity of exercise is decreased (Helgerud *et al.* 2007). Cardiac muscle cells become hypertrophied in response to mechanical, hormonal, pathological, and hemodynamic stimuli to adapt to the demand in the myocardium (Nakamura and Sadoshima 2018). Until now, the molecular mechanisms responsible for exercise-induced CH are not fully understood.

miRNAs are small, non-coding RNAs of 8–24 nucleotides in length and are diagnostic and therapeutic targets for many diseases. miRNAs play a significant role in regulating CH and fibrosis (Chen *et al.* 2017; Nakamura and Sadoshima 2018). Mature miRNAs carry out target regulation by two distinct mechanisms: suppression of mRNA translation and degradation of mRNA. miRNAs are introduced into circulation by exosomes, protein complexes, and microvesicles. Packaged transport of miRNAs protects them from cellular degradation and enables them to reach their destination (Barber *et al.* 2019). Circulating miRNAs are used as biomarkers in the diagnosis of many diseases.

Studies are needed in experimental animals to understand the molecular mechanisms of exercise-induced CH. Experimental models usually use rats and mice. Treadmill, wheel spin, and swimming exercise models are applied to these animals. Swimming, treadmill, or wheel spinning exercises are equally effective in creating physiological hypertrophy (Wang *et al.* 2010). Insulin-like growth factor (IGF-1), phosphoinositide 3-kinase, protein kinase B, the mechanical target of rapamycin (PI3/Akt/mTOR), a mitogen-activated protein kinase (MAPK), and tumor protein p53 (p53) signaling pathways cause physiological CH. Activation or inactivation of the Akt/mTOR signaling pathway differs in physiological and pathological hypertrophy. This study aims to identify miRNAs that play a role in CH which develops in response to swimming exercise. We aimed to evaluate the target genes of these miRNAs by bioinformatic analysis and to show the roles of these genes in the CH signaling pathway. We also searched for miRNAs in the blood that might indicate cardiac fibrosis. Thus, we can define a biomarker that can show sudden cardiac death in young athletes.

2. Materials and methods

2.1 Animal model of exercise-induced cardiac hypertrophy

As the rat's heart resembles the human heart (Wang *et al.* 2010), it is advantageous in mimicking human diseases in terms of myocardium structure and growth pattern (although the direction of contraction is different from humans). Fifteen male Sprague–Dawley rats weighing 300–350 g were used as subjects. Three to five rats were housed per cage at controlled room temperature (22°C) with a 12 h dark–light cycle and fed standard rat chow *ad libitum*. Rats were randomly divided into two groups: control group (CG, $n=6$) and training group (TG, $n=9$). The control group remained in their cage throughout the study. This study was approved by the Experimental Animals Ethics Committee (approval number: 2014/159), and the experiments were conducted in accordance with the international guidelines on the ethical use of animals.

2.2 Exercise protocol

The swimming exercise model was used to generate CH by aerobic exercise and the swimming exercise was performed in a cylindrical glass beaker filled with water, ~35 cm deep and 50 cm wide. The beakers were maintained in a thermostatic water bath between 30°C and 32°C. In the TG, rats were habituated to swimming for 20 min a day. The exercise time was gradually increased by 10 min per day up to 60 min a day. Swimming sessions of 60 min duration were performed for 5 days a week, for 8 weeks. In the 9th week, the rats swam twice a day, and in the 10th week, the rats swam thrice a day, with sessions of 60 min duration (Soci *et al.* 2011). The procedure lasted for 10 weeks. Rats swam simultaneously in groups of 4–5.

Echocardiography was performed on both groups of rats before and after the exercise program to assess cardiac structure and function under ketamine (45 mg/kg) and xylazine (5 mg/kg) anesthesia (Kawahara *et al.* 2005).

2.3 Echocardiography

Echocardiographic measurements were recorded using a Philips HD7 XE ultrasound system with an S12-4 transducer (Philips Medical Systems, Andover, Massachusetts). Measurements were obtained in M-mode

and Doppler (scanning at 100 or 150 mm/s). Measurements were conducted according to the principles accepted by the American Society of Echocardiography (Quiñones *et al.* 2002). The rats were anesthetized with ketamine (45 mg/kg) and xylazine (5 mg/kg) intraperitoneally. Under anesthesia, the breasts of the animals were shaved and placed in the left lateral decubitus position. Short-axis, two-dimensional images of the left ventricle were taken at the level of the papillary muscles. Ventricular septum (IVS) thickness, posterior wall thickness (LPWT), left ventricular systolic and diastolic inner dimensions (LVDs and LVDd), and left ventricular ejection fraction (LVEF) were measured from three consecutive cardiac cycles with a M-mode recorder. Left ventricular mass was calculated according to the formula: $LV\ mass = 1.04 \times [(LVDd + LVPW + IVS)^3 - LVDd^3]g$ (Simone *et al.* 1990).

2.4 Surgery of cardiac tissue

After the exercise program, blood samples were obtained by intracardiac puncture under anesthesia. Then, the blood samples were taken into EDTA blood collection tubes, kept at room temperature for 10 min and centrifuged at 3000 rpm for 10 min, and the serum was collected. Serum samples were aliquoted into three different DNAase-RNase-free tubes and stored at -80°C until the analysis of miRNA expression. Further, the heart tissue was removed. To prevent RNA degradation, the heart tissue was aliquoted and stored in a liquid nitrogen tank. Some of the heart tissues were stored in 10% formaldehyde until histological analysis.

2.5 Prediction and bioinformatic analysis for validation of miRNAs

miRNAs are epigenetic tools used in the diagnosis and treatment of human diseases. The tissue-specific expression (limited number) and multiple targets of miRNAs limit the research. For this reason, it is essential to select the target tissue and interpret the results correctly. The miRNA sequences in the rat genome show homology with the miRNA sequences in the human genome, which provides an advantage in our planned studies.

In this study, we investigated the miRNAs showing homology between the two species using the miRNAminer database (<http://pag.csail.mit.edu/mirnaminer>) (Artzi *et al.* 2008). We selected miRNAs

Table 1. Selected miRNAs and specific primer sequences

| miRNA names | Specific primer sequence |
|-------------------|--------------------------|
| rno-miR-98-5p | GAGGTAGTAAGTTGTATTGT |
| rno-miR-106b-5p | AAAGTGCTGACAGTGCAGA |
| rno-miR-132-3p | AACAGTCTACAGCCATGGTC |
| rno-miR-192-5p | TGACCTATGAATTGACAGC |
| rno-miR-194-5p | GTAACAGCAACTCCATGTGG |
| rno-miR-290 | TCTCAAACCTATGGGGGCA |
| rno-miR-350 | CACAAAGCCCATACACTTTC |
| rno-miR-466b-2-3p | TATACATACACACATACAC |
| rno-miR-6322 | CAGGGACTGCAAGGAGCCG |

with high homology according to microRNAviewer (<http://people.csail.mit.edu/akiezun/microRNAviewer/>). miRNAs in metabolic pathways associated with CH were screened using the mirPath database and the KEGG pathway, and miRNAs that provided this matching were preferred for array analysis. According to the results of the array, downregulated and upregulated miRNAs were searched in the miRDB database (Liu and Wang 2019; Chen and Wang 2020) and miRNAs with the highest target specificity were selected. The predicted target genes were evaluated using the KEGG orthology-based annotation system and the Qiagen Inventive Pathway Analysis system (IPA) (Krämer et al. 2014).

Targets of miRNAs were determined using miRNet (<https://www.mirnet.ca>). miRNA-target gene ontology analysis was performed and evaluated using miRBase (http://mirbase.org/cgi-bin/mature.pl?mature_acc=MIMAT0000426) (Release 22.1: October 2018). Finally, potential target genes of miRNAs whose activities are altered in CH were determined by

comparative analysis of the human and rat genome (https://www.disgenet.org/browser/0/1/0/C1383860/25/100/source__ALL/_b./).

2.6 Array analysis of miRNA expressions in cardiac tissue and blood serum RNA extraction

The homogenization of heart tissues (50 mg) was done using ceramic bead tubes DNase-RNase-free (MP Biomedicals, CA, USA). Total RNA was isolated from the obtained homogenate using the kit protocol (GenUP™ Total RNA Kit, BR0700902). For the analysis of circulating miRNAs, 400 µL serum sample was taken and the total RNA was isolated according to the same kit protocol. The amount and purity of total RNAs obtained from both tissue and serum samples were measured using a spectrophotometer (NanoDrop 8000, DE 19810, Thermo Fisher, USA). The amount of RNA in the isolated samples was calculated according to the formula given below (Barbas et al. 2007). In addition, the purity of the RNA was determined using the OD260/OD280 ratio (C indicates purity).

$$C (\mu\text{g/mL}) = (\text{OD260}) \times 40$$

A pool was created from the isolated RNAs for microarray analysis. The pool was created from total RNA obtained from the heart tissues of rats in the TG and CG, by mixing 100 ng/µL RNA in a tube for each group. Whole-genome analysis of miRNA expressions from *Rattus norvegicus* was performed with the Affymetrix microarray system (Affymetrix miRNA 4.0 and miRNA 2.0, Ayka Ltd, Ankara, Turkey) (1250 miRNA for miRNA 4.0, 778 miRNA

Table 2. Evaluation of cardiac functions with electrocardiography in exercise and control group rats

| Parameters | CG (n=6) | | TG (n=8) | |
|------------|-------------------|------------------|-----------------------------|----------------|
| | First measurement | Last measurement | Before exercise | After exercise |
| Weight (g) | 388.00 ± 26.42* | 411.67 ± 30.02 | 384.63 ± 8.78* ^Δ | 352.38 ± 20.74 |
| IVS (mm) | 1.59 ± 0.07 | 1.58 ± 0.08 | 1.55 ± 0.13* | 1.60 ± 0.14 |
| LPWT (mm) | 1.61 ± 0.10 | 1.61 ± 0.09 | 1.57 ± 0.12* | 1.61 ± 0.14 |
| LVDd (mm) | 5.24 ± 0.25 | 5.25 ± 0.32 | 4.70 ± 0.33* ^{ΔΔ} | 4.91 ± 0.31 |
| LVDs (mm) | 2.82 ± 0.32 | 2.85 ± 0.41 | 2.55 ± 0.39* | 2.70 ± 0.35 |
| LVmass (g) | 0.47 ± 0.01 | 0.47 ± 0.02 | 0.38 ± 0.06* ^Δ | 0.43 ± 0.07 |
| LVEF (%) | 76.88 ± 5.48 | 76.05 ± 7.38 | 76.59 ± 8.01* | 75.81 ± 5.97 |

IVS, interventricular septum thickness; LPWT, left posterior wall thickness; LVDd, left ventricular diastolic dimension; LVDs, left ventricular systolic dimension; LVmass, left ventricular mass index; LVEF, left ventricular ejection fraction. Here, $p < 0.05$ were considered significant. Here $n=8$ because of the death of a rat in electrocardiography measurement after the exercise program.

*Within groups; ^Δbetween groups; *^Δ $p < 0.05$; *^{ΔΔ} $p < 0.01$.

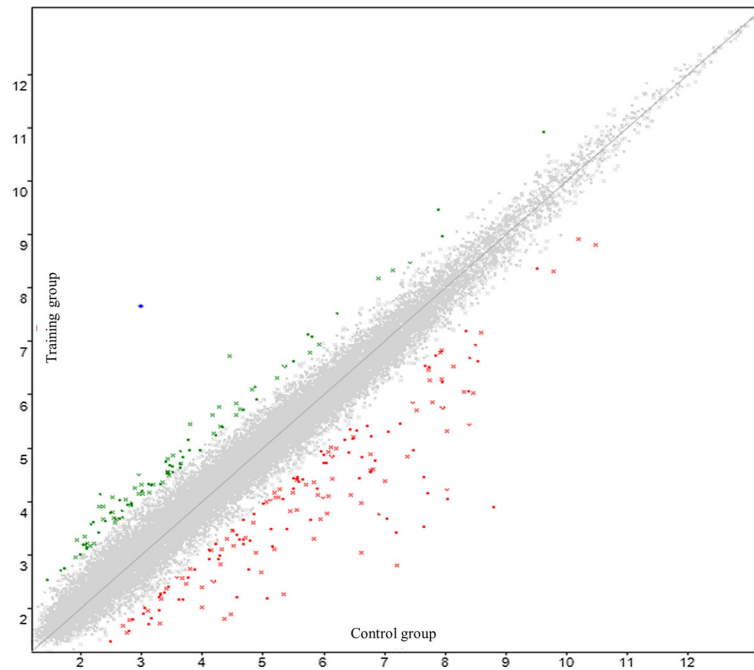


Figure 1. Scatter plot of miRNA microarray analysis which was visualized to express the variation between chips. The axes of the scatter plot are the normalized signal data of the exercise and control group samples.

for miRNA 2.0) (Thermo Fisher, GeneChipTM miRNA 4.0 Array 902411; GeneChipTM miRNA 2.0 Array 901755). For the analysis of the expression of miRNAs from tissue and serum samples, complementary DNA (cDNA) was obtained from total RNA using the kit (qScriptTM microRNA Synthesis Kit-VWR) protocol.

2.7 cDNA analysis with reverse transcriptase-PCR

In the first step, the polyA tail was added to the miRNAs obtained from the samples. The total reaction volume was made up of 10 μ L: 2 μ L 5 \times poly(A) tailing buffer, 1 μ L pol (A) polymerase, 4 μ L nuclease-free water, and 3 μ L total RNA. Subsequently, samples were incubated in a thermal cycler (T100TM Thermal Cycler, Bio-Rad, California, USA) at 37°C for 1 h, 1 cycle, and at 70°C for 5 min, 1 cycle. In the second step, the cDNA was obtained. For this, a 20 μ L volume was created by adding RNA and miRNA-cDNA reaction mix to the 10 μ L mixture in the first step: 10 μ L poly(A) RNA, 9 μ L miRNA-cDNA reaction mix, and 1 μ L qScript reverse transcriptase. Following this process, the sample was incubated in the thermal cycler at 42°C for 20 min, 1 cycle, and at 85°C for 5 min, 1 cycle (reverse transcriptase-PCR). In the third

step, miRNA expressions were analyzed by real-time PCR (CFX ConnectTM, Bio-Rad, Richmond, CA) using the *U6* gene, a housekeeping gene, as an endogenous control for the relative analysis of miRNA measurements in tissues (Masè *et al.* 2017). The reaction mixture was prepared as a total volume of 20 μ L, containing 10 μ L 2 \times SYBR Green SuperMix, 0.4 μ L forward primer (rat *U6* for tissue endogenous control), 0.4 μ L reverse primer (Universal PCR primer), 8.2 μ L nuclease-free water, and 1 μ L template (cDNA). Finally, the reaction mixture was prepared for 2 min pre-incubation/activation (1 cycle) at 95°C, 5 s, for denaturation at 95°C, 15 s, for annealing at 60°C, 15 s, for the extension at 70°C (40 cycles). By performing melting curve analysis in the extension step, real-time PCR was programmed to make a reading from 70°C to 90°C in 0.2 s with 0.5°C increments. By using the obtained cDNAs, the downregulation and upregulation of miRNAs were determined by real-time PCR. Validation of miRNA expression was by quantitative real-time PCR (qRT-PCR). Analyses were conducted using the BIORAD-CFX Connect real-time PCR system and the Perfecta[®] SYBR Green FastMix[®] Reaction Mixes-VWR kit. Of the 128 miRNAs associated with CH, the validation of nine miRNAs that met the criteria previously mentioned was performed. The expression of miRNAs in cardiac tissue and serum samples was accurately detected by microarray (Affymetrix, Thermo

Table 3. Arrays of miRNAs and their accession numbers

| miRNA name | Fold change | Regulation | Accession number |
|------------------------|--------------|-------------|------------------|
| rno-miR-194-5p | 15.5 | Upregulated | MIMAT0000869 |
| rno-miR-350 | 13.22 | Upregulated | MIMAT0000604 |
| rno-miR-132-3p | 11.26 | Upregulated | MIMAT0000838 |
| rno-miR-98-5p | 10.26 | Upregulated | MIMAT0000819 |
| rno-miR-192-5p | 9.49 | Upregulated | MIMAT0000867 |
| rno-miR-106b-5p | 6.13 | Upregulated | MIMAT0000825 |
| rno-miR-21-5p | 5.78 | Upregulated | MIMAT0000790 |
| rno-miR-140-5p | 5.69 | Upregulated | MIMAT0000573 |
| rno-miR-34a-5p | 5.52 | Upregulated | MIMAT0000815 |
| rno-miR-20a-5p | 5.04 | Upregulated | MIMAT0000602 |
| rno-miR-19b-3p | 4.64 | Upregulated | MIMAT0000788 |
| rno-miR-24-2-5p | 4.63 | Upregulated | MIMAT0005441 |
| rno-miR-28-5p | 4.61 | Upregulated | MIMAT0000800 |
| rno-miR-30e-5p | 4.6 | Upregulated | MIMAT0000805 |
| rno-miR-339-5p | 4.56 | Upregulated | MIMAT0000583 |
| rno-miR-499-5p | 4.44 | Upregulated | MIMAT0003381 |
| rno-miR-450a-5p | 4.34 | Upregulated | MIMAT0001547 |
| rno-miR-490-3p | 4.34 | Upregulated | MIMAT0012823 |
| rno-miR-872-3p | 4.3 | Upregulated | MIMAT0005283 |
| rno-miR-125b-2-3p | 4.26 | Upregulated | MIMAT0026467 |
| rno-miR-1839-5p | 4.2 | Upregulated | MIMAT0024843 |
| rno-miR-27a-3p | 4.11 | Upregulated | MIMAT0000799 |
| rno-miR-26b-5p | 4.08 | Upregulated | MIMAT0000797 |
| rno-miR-7a-1-3p | 4.06 | Upregulated | MIMAT000607 |
| rno-miR-29b-2-3p | 4.03 | Upregulated | MIMAT0004717 |
| rno-miR-22-5p | 4 | Upregulated | MIMAT00003152 |
| rno-miR-15b-5p | 3.96 | Upregulated | MIMAT0000784 |
| rno-miR-17-5p | 3.91 | Upregulated | MIMAT0000786 |
| rno-miR-106b-3p | 3.89 | Upregulated | MIMAT00004727 |
| rno-miR-451-5p | 3.81 | Upregulated | MIMAT0001633 |
| rno-miR-503-3p | 3.79 | Upregulated | MIMAT0017224 |
| rno-miR-342-3p | 3.77 | Upregulated | MIMAT0000589 |
| rno-miR-133a-5p | 3.75 | Upregulated | MIMAT0017124 |
| rno-miR-185-5p | 3.72 | Upregulated | MIMAT0000862 |
| rno-miR-345-3p | 3.7 | Upregulated | MIMAT0004655 |
| rno-miR-101b-3p | 3.61 | Upregulated | MIMAT0000615 |
| rno-miR-10a-5p | 3.6 | Upregulated | MIMAT0000782 |
| rno-miR-30b-5p | 3.56 | Upregulated | MIMAT0000806 |
| rno-miR-27b-3p | 3.55 | Upregulated | MIMAT0000798 |
| rno-miR-374-5p | 3.55 | Upregulated | MIMAT0003208 |
| rno-miR-532-5p | 3.55 | Upregulated | MIMAT0005322 |
| rno-miR-20b-5p | 3.49 | Upregulated | MIMAT0003221 |
| rno-miR-30c-1-3p | 3.4 | Upregulated | MIMAT0004719 |
| rno-miR-425-5p | 3.38 | Upregulated | MIMAT0005314 |
| rno-miR-143-3p | 3.36 | Upregulated | MIMAT0000849 |
| rno-miR-146b-5p | 3.35 | Upregulated | MIMAT0005595 |
| rno-miR-184 | 3.34 | Upregulated | MIMAT0000861 |
| rno-miR-29c-3p | 3.33 | Upregulated | MIMAT0000803 |
| rno-miR-301a-3p | 3.3 | Upregulated | MIMAT0000552 |
| rno-miR-200b-3p | 3.3 | Upregulated | MIMAT0000875 |
| rno-miR-503-5p | 3.3 | Upregulated | MIMAT0003223 |
| rno-miR-322-5p | 3.24 | Upregulated | MIMAT0001619 |
| rno-miR-30c-2-3p | 3.21 | Upregulated | MIMAT0005442 |
| rno-miR-29c-5p | 3.1 | Upregulated | MIMAT0003154 |
| rno-miR-423-5p | 3.03 | Upregulated | MIMAT0017305 |
| rno-miR-30a-5p | 2.99 | Upregulated | MIMAT0000808 |
| rno-miR-30a-3p | 2.98 | Upregulated | MIMAT0000809 |

Table 3 (continued)

| miRNA name | Fold change | Regulation | Accession number |
|-------------------|-------------|-------------|------------------|
| rno-miR-199a-5p | 2.96 | Upregulated | MIMAT0000872 |
| rno-miR-29b-3p | 2.93 | Upregulated | MIMAT0000801 |
| rno-miR-322-3p | 2.92 | Upregulated | MIMAT0000547 |
| rno-miR-181c-5p | 2.9 | Upregulated | MIMAT0000857 |
| rno-miR-28-3p | 2.88 | Upregulated | MIMAT0004716 |
| rno-miR-93-5p | 2.86 | Upregulated | MIMAT0000817 |
| rno-miR-511-3p | 2.86 | Upregulated | MIMAT0017358 |
| rno-miR-148b-3p | 2.79 | Upregulated | MIMAT0000579 |
| rno-miR-7a-5p | 2.74 | Upregulated | MIMAT0000606 |
| rno-miR-24-3p | 2.66 | Upregulated | MIMAT0000794 |
| rno-miR-222-3p | 2.63 | Upregulated | MIMAT0000891 |
| rno-miR-352 | 2.61 | Upregulated | MIMAT0000610 |
| rno-miR-532 | 2.6 | Upregulated | MI0006154 |
| rno-miR-151-5p | 2.59 | Upregulated | MIMAT0000613 |
| rno-miR-25-3p | 2.59 | Upregulated | MIMAT0000795 |
| rno-miR-30d-5p | 2.56 | Upregulated | MIMAT0000807 |
| rno-miR-152-3p | 2.51 | Upregulated | MIMAT0000854 |
| rno-miR-122-5p | 2.49 | Upregulated | MIMAT0000827 |
| rno-miR-195-5p | 2.46 | Upregulated | MIMAT0000870 |
| rno-miR-30c-5p | 2.45 | Upregulated | MIMAT0000804 |
| rno-miR-100-5p | 2.38 | Upregulated | MIMAT0000822 |
| rno-miR-130a-3p | 2.35 | Upregulated | MIMAT0000836 |
| rno-miR-181d-5p | 2.35 | Upregulated | MIMAT0005299 |
| rno-miR-107-3p | 2.34 | Upregulated | MIMAT0000826 |
| rno-miR-378a-3p | 2.34 | Upregulated | MIMAT0003379 |
| rno-miR-191a-5p | 2.33 | Upregulated | MIMAT0000866 |
| rno-miR-351-5p | 2.32 | Upregulated | MIMAT0000608 |
| rno-miR-16-5p | 2.32 | Upregulated | MIMAT0000785 |
| rno-miR-128-3p | 2.32 | Upregulated | MIMAT0000834 |
| rno-miR-let-7i-5p | 2.31 | Upregulated | MIMAT0000779 |
| rno-miR-378b | 2.29 | Upregulated | MIMAT0024855 |
| rno-miR-497-5p | 2.28 | Upregulated | MIMAT0003383 |
| rno-miR-344a-2 | 2.28 | Upregulated | MI0015432 |
| rno-miR-212-3p | 2.25 | Upregulated | MIMAT0000883 |
| rno-miR-1839-3p | 2.25 | Upregulated | MIMAT0024844 |
| rno-miR-99a-5p | 2.24 | Upregulated | MIMAT0000820 |
| rno-miR-26a-5p | 2.23 | Upregulated | MIMAT0000796 |
| rno-miR-155-5p | 2.23 | Upregulated | MIMAT0030409 |
| rno-miR-22-3p | 2.22 | Upregulated | MIMAT0000791 |
| rno-miR-30b-3p | 2.21 | Upregulated | MIMAT0004721 |
| rno-miR-146a-5p | 2.21 | Upregulated | MIMAT0000852 |
| rno-miR-532-3p | 2.21 | Upregulated | MIMAT0005323 |
| rno-miR-30e-3p | 2.2 | Upregulated | MIMAT0004720 |
| rno-miR-103-3p | 2.2 | Upregulated | MIMAT0000824 |
| rno-miR-126a-3p | 2.19 | Upregulated | MIMAT0000832 |
| rno-miR-361-5p | 2.18 | Upregulated | MIMAT0003117 |
| rno-miR-324-5p | 2.17 | Upregulated | MIMAT0000553 |
| rno-miR-221-3p | 2.16 | Upregulated | MIMAT0000890 |
| rno-miR-let-7f-5p | 2.12 | Upregulated | MIMAT0000778 |
| rno-miR-199a-3p | 2.12 | Upregulated | MIMAT0004738 |
| rno-miR-27b-5p | 2.11 | Upregulated | MIMAT0017101 |
| rno-miR-127-3p | 2.11 | Upregulated | MIMAT0000833 |
| rno-miR-208a-5p | 2.09 | Upregulated | MIMAT0017155 |
| rno-miR-125a-3p | 2.07 | Upregulated | MIMAT0004729 |
| rno-miR-140-3p | 2.06 | Upregulated | MIMAT0000574 |
| rno-miR-19a-3p | 2.06 | Upregulated | MIMAT0000789 |
| rno-miR-29a-3p | 2.06 | Upregulated | MIMAT0000802 |

Table 3 (continued)

| miRNA name | Fold change | Regulation | Accession number |
|--------------------------|--------------|---------------|------------------|
| rno-miR-145-3p | 2.06 | Upregulated | MIMAT0017131 |
| rno-miR-23a-3p | 2.05 | Upregulated | MIMAT0000792 |
| rno-miR-92a-3p | 2.05 | Upregulated | MIMAT0000816 |
| rno-miR-25 | 2.04 | Upregulated | MI0000856 |
| rno-miR-6324 | -2.05 | Downregulated | MIMAT000025063 |
| rno-miR-326-5p | -2.09 | Downregulated | MIMAT0017028 |
| rno-miR-935 | -2.09 | Downregulated | MI0012607 |
| rno-miR-92b-3p | -2.1 | Downregulated | MIMAT0005340 |
| rno-miR-365-5p | -2.35 | Downregulated | MIMAT0017184 |
| rno-miR-6332 | -2.41 | Downregulated | MIMAT0025073 |
| rno-miR-290 | -2.42 | Downregulated | MIMAT0000893 |
| rno-miR-667-3p | -2.79 | Downregulated | MIMAT0012852 |
| rno-miR-466b-2-3p | -3.67 | Downregulated | MIMAT0017286 |

Accession numbers belong to mirbase database (<http://www.mirbase.org>). Selected miRNAs are expressed in bold.

Fisher Scientific, ABD) (Rat Gene.2.0 ST Array). Microarray results were verified by the real-time quantification method using System Biosciences (SBI). Nine miRNAs and specific primer sequences selected to test differential expression analysis are given in table 1.

RT-PCR amplifications were performed using Sybr Green PCR Master mix (Perfecta® SYBR Green FastMix® Reaction Mixes-VWR, Beverly, California) with the BIORAD-CFX Connect RT-PCR system. Thermal cycling conditions were programmed for 10 min at 95°C, followed by 5 s at 95°C, 15 s at 60°C, and 15 s at 70°C for 40 cycles. Each sample was analyzed in duplicate. Samples were standardized by *U6* endogenous control (Δ CT). The relative quantification of the standardized samples was calculated by the $2^{-\Delta\Delta CT}$ method (Livak and Schmittgen 2001).

2.8 Histological analysis of heart tissue

Heart tissues were fixed in 10% formalin and were embedded in paraffin, following the routine tissue preparation processes. The embedded tissues were cut as 4 μ m sections. Hemotoxylin & Eosin (HE) and Masson Trichrome techniques were used to observe heart tissue cell morphology. All samples were evaluated for cardiomyocyte hypertrophy, myofibrillary disorder, and interstitial fibrosis. Myocytes were considered hypertrophied if they had consistently enlarged and hyperchromatic nuclei and their cell diameter was >20 μ m or greater than the diameter of three red blood cells (RBCs). Myofibrillar disorder included cellular

interlacing, rotation, or herringbone patterns (Maron *et al.* 1992). Therefore, hypertrophy was generally considered mild if myocyte diameters were 21 to 29 μ m (3–4 RBCs), moderate if 30 to 38 μ m (4–5 RBCs), and severe if >38 μ m (>5 RBCs). The severity of interstitial fibrosis was scored by examining samples stained with the Masson Trichrome method. In the absence of interstitial fibrosis, it was classified as grade 0 (<5%), mild interstitial fibrosis as grade 1 (6–15%), moderate interstitial fibrosis as grade 2 (16–25%), and advanced interstitial fibrosis as grade 3 (>25%). Enlarged and hyperchromatic nuclei and enlarged cells were examined to reveal cardiomyocyte hypertrophy. In addition, scoring was done by taking into account necrosis, bleeding, and intercellular edema. Each sample was scored as 0=negative, 1=mild, 2=moderate, or 3=severe to evaluate histopathological changes in the heart muscle and fibers. A Nikon Eclipse i5 light microscope was used for the histopathological study based on the Kiernan protocol (Kiernan 1999). Areas in tissues were analyzed and quantified using the intelligent segmentation feature in the Nikon NIS Elements version 4.0 image analysis system (Nikon Instruments Inc., Tokyo, Japan). The histologist and pathologist studied the slides in a single blind protocol.

2.9 Detection of apoptosis with the TUNEL test

A TUNEL (terminal deoxynucleotidyl transferase-mediated dUTP nick end labeling) kit (Roche - 11 684 795 910) was used to evaluate apoptosis in the heart tissue. The heart tissue fixed in 10% formalin was embedded

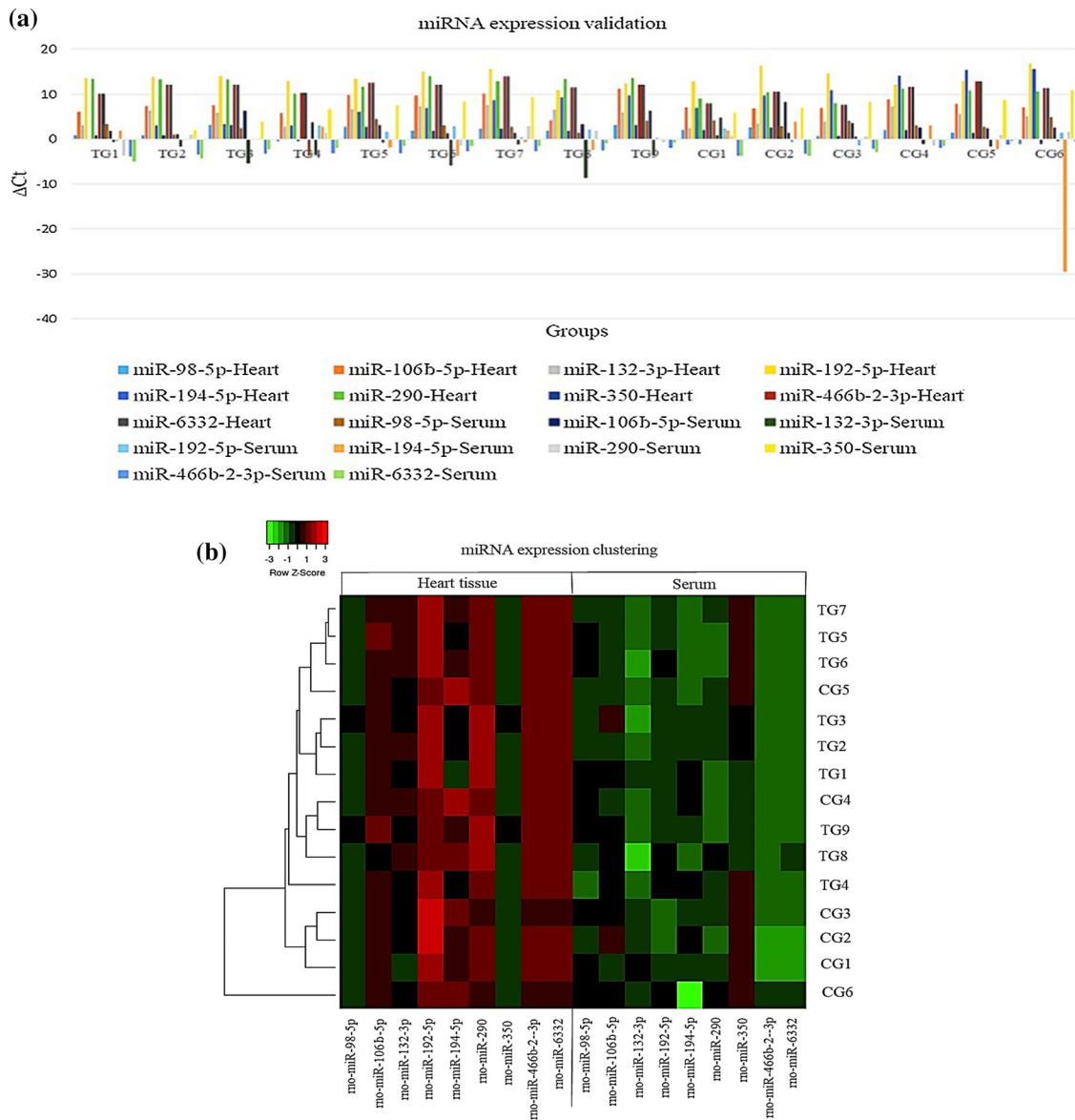


Figure 2. (a) Nine miRNA expression profiles of the heart tissue and serum. (b) Heatmap of miRNA expression profiles in the heart tissue and serum in exercise-induced cardiac hypertrophy determines clustering in tissue difference and exercise miRNA expression. Three replicates and tissue clusters from each stage are shown. The green color indicates expression downregulated from the mean and the red color indicates expression upregulated from the mean. Columns and rows represent samples (TG and CG), respectively, and nine miRNAs in both tissues.

in paraffin and sectioned. Then, according to the instructions of the TUNEL kit, apoptosis was evaluated and scored as no (–), mild (+), moderate (++), and severe (+++) (Mokhtari *et al.* 2015) by randomly selecting 10 fields of view.

2.10 Determination of proliferation of heart tissue cells

The Histostain™-Plus proliferative cell nuclear antigen (PCNA) staining kit was used for the

immunohistochemical detection of nuclear antigens of proliferating cells (Invitrogen, 93-1143). Sections were incubated at room temperature with the labeled streptavidin-peroxidase method (Histostain®-Plus kit Zymed) according to the kit protocol. Samples were treated with biotinylated mouse anti-PCNA primary antibody and stained with hematoxylin. The results were examined with a light microscope using a Zeiss Axioplan 2 microscope. Immunopositivity was scored according to staining intensity (I) and percentage of positive cells (P). The staining intensity was rated as follows; 0, undetectable; 1, bad coloring; 2, medium

Table 4. Nine miRNA expression levels in TG and CG groups: Analysis of variance of miRNA expression data in heart tissue and serum for association with CH

| Tissue | miRNA | CG (<i>n</i> =6) | | TG (<i>n</i> =9) | | <i>p</i> -Value |
|--------|------------------------|-------------------------|----------------------|-------------------------|---------------------|-----------------|
| | | Median expression value | 25–75% | Median expression value | 25–75% | |
| Heart | rno-miR-98-5p | 1.27 | [1.97–1.03] | 1.79 | [0.80–3.13] | 0.449 |
| | rno-miR-106b-5p | 3.59 | [2.81–4.93] | 2.06 | [0.99–3.98] | 0.615 |
| | rno-miR-132-3p | 4.75 | [2.39–7.18] | 5.76 | [2.69–7.58] | 0.254 |
| | rno-miR-192-5p | 14.20 | [12.01–16.71] | 13.46 | [10.86–15.49] | 0.403 |
| | rno-miR-194-5p | 5.55 | [3.06–9.68] | 12.09 | [6.99–15.57] | 0.003 |
| | rno-miR-290 | 12.74 | [10.08–13.93] | 9.98 | [8.02–11.13] | 0.004 |
| | rno-miR-350 | 1.27 | [–1.03–2.60] | 1.79 | [–0.55–3.19] | 0.449 |
| | rno-miR-466b-2-3p | 10.33 | [7.94–12.82] | 11.82 | [10.11–13.97] | 0.094 |
| | rno-miR-6332 | 10.28 | [7.86–12.10] | 11.95 | [10.08–14.36] | 0.087 |
| Serum | rno-miR-98-5p | 3.59 | [2.81–4.93] | 2.06 | [0.99–3.98] | 0.402 |
| | <i>rno-miR-106b-5p</i> | 3.38 | [0.77–8.30] | 3.18 | [1.170–6.42] | 0.987 |
| | rno-miR-132-3p | –3.47 | [–8.69–0.60] | 0.58 | [–1.71–4.83] | 0.045 |
| | rno-miR-192-5p | 0.32 | [–1.40–2.28] | 1.09 | [–0.32–3.00] | 0.557 |
| | rno-miR-194-5p | 0.32 | [–29.51–3.90] | 1.09 | [–3.690–2.65] | 0.820 |
| | rno-miR-290 | 0.43 | [0.70–1.58] | 0.18 | [–3.68–2.85] | 0.976 |
| | rno-miR-350 | 8.14 | [5.99–10.89] | 5.36 | [–0.22–9.35] | 0.365 |
| | rno-miR-466b-2-3p | –2.11 | [–3.63–0.50] | –2.94 | [–3.87–1.93] | 0.251 |
| | rno-miR-6332 | –2.02 | [–3.69–0.04] | –2.20 | [–4.97–0.83] | 0.975 |

$p < 0.05$ were considered significant for miRNA expression changes between TG patients and CG samples. Boldface indicates statistical significance. The median (50th percentile), first quartile (25th percentile), and third quartile (75th percentile) are reported here. However, with nine miRNA expression data serving as predictor variables, we note that the miR-194-5p significance level ($p = 0.003$) and miR-290 significance level ($p = 0.004$) in the heart tissue, and miR-132-3p significance level ($p = 0.045$) in the serum would still survive correction for multiple testing (where significant, $p < 0.01$). *n*, Numbers of animals; TG, training group; CG, control group.

staining; and 3, heavy staining. All positive cells in the fields were evaluated. Each rat was calculated by the Quick Score (Q) in which the percentage of positive cells (P) was multiplied by the intensity (I), using the formula: $Q = P \times I$, resulting in a score between 0 and 300 (Mega *et al.* 2014). The final score for each group was taken as the mean.

2.11 Statistical analysis

In the analysis of echocardiographic measurements, for the exercise and control groups, the Wilcoxon–Whitney U-test was used for in-group comparisons and the Mann–Whitney U-test was used to show differences between groups. For the statistical analysis of genes whose expressions were determined in blood and heart tissues obtained from both groups, the Wilcoxon–Whitney and Mann–Whitney U-tests were used as non-parametric tests. The Mann–Whitney U-test was used to determine the

significance of histopathological changes in the heart tissue. Results are presented as the median (50th percentile), first quartile (25th percentile), and third quartiles. Statistically, $p < 0.05$ was considered significant. The ROC curve was drawn, and AUC was assessed for the specificity and sensitivity of miRNAs. The data were analyzed using the statistical package SPSS (Release 11.5, SPSS Inc, Chicago, IL, USA) for Windows.

3. Results

In this study, the expression of miRNAs in CH developed in swimming exercise group of rats was examined by microarray analysis and then confirmed by qPCR. Expression profiles of two different tissues (heart and serum) were obtained and visualized histologically and pathologically. This study provided information about miRNAs whose activities are altered in circulation and heart tissue.

Table 5. Differentially expressed (fold change>0.05) miRNAs in exercise-induced CH

| miRNA name | Fold change | Regulation | Tissue type |
|-------------------|---------------|---------------|-------------|
| rno-miR-98-5p | 1.434 | Upregulated | Heart |
| rno-miR-106b-5p | 1.435 | Downregulated | |
| rno-miR-132-3p | 2.013 | Upregulated | |
| rno-miR-192-5p | 0.599 | Downregulated | |
| rno-miR-194-5p | 92.766 | Upregulated | |
| rno-miR-290 | 6.795 | Downregulated | |
| rno-miR-350 | 1.434 | Upregulated | Serum |
| rno-miR-466b-2-3p | 2.818 | Upregulated | |
| rno-miR-6332 | 2.818 | Upregulated | |
| rno-miR-98-5p | 0.346 | Downregulated | |
| rno-miR-106b-5p | 0.871 | Downregulated | |
| rno-miR-132-3p | 0.060 | Upregulated | |
| rno-miR-192-5p | 1.707 | Upregulated | |
| rno-miR-194-5p | 15.224 | Upregulated | |
| rno-miR-290 | 0.840 | Downregulated | |
| rno-miR-350 | 0.145 | Downregulated | |
| rno-miR-466b-2-3p | 0.562 | Downregulated | |
| rno-miR-6332 | 0.880 | Downregulated | |

Differentially expressed (fold change) miRNAs are expressed in bold.

3.1 Electrocardiographic measurement

In this study, the first of the follow-up indicators of hypertrophic development was the echocardiographic measurements performed before and after the exercise program. When the TG group was compared within the group and between the CG group, significant increases were found in the LVmass, the LVDD, the LVDs, LPWT, and the IVS in TG (table 2).

3.2 Affymetrix 4.0 and 2.0 miRNA microarray

The whole genome (25,000 genes) of rats in TG and CG was evaluated by microarray analysis. All 128 miRNAs associated with CH were identified (table 2; figure 1).

3.3 Expression levels of miRNAs in heart tissue and serum samples

Considering the fold change ≥ 2 and $p < 0.05$ values obtained from the microarray analysis and the bioinformatics analyses in the databases, a total of nine miRNAs, of which the six most upregulated miRNAs (miR-194-5p, miR-350, miR-132-3p, miR-98-5p, miR-192-5p, miR-106b-5p), and three of the most downregulated miRNAs (miR-466b-2-3p, miR-290, miR-

6332) were preferred for expression analysis by real-time PCR validation. The expression profile of each miRNA was evaluated by a single factor ANOVA test. It provided p -values ranging from 0.003 to 0.987, indicating that the results were statistically significant in heart tissue and serum for three miRNAs (see table 3 and figure 2a for specific comparisons). Microarray analysis results of miRNAs expressed in two different tissues are presented in figure 1 as a scatter plot. In all of the probes shown in figure 1, the p -values of two miRNAs in heart tissue and one miRNA in serum were highly significant ($p < 0.05$). In the heart tissue of the TG, miR-194-5p expression increased ($p = 0.003$) and miR-290 expression decreased ($p = 0.004$). MiR-132-3p expression increased in the serum sample of the TG ($p = 0.045$) (table 4). In heart tissue, six miRNAs were upregulated while three miRNAs were downregulated. In serum, three miRNAs were upregulated and six miRNAs were downregulated (table 5). The important result was that the expression of the five miRNAs (miR-192-5p, -194-5p, -290, -466b-2-3p, -6332) in heart tissue was much higher and statistically significant than in serum ($F = 14,069$, $df = 1$, $p = 0.018$) (figure 2b). These results suggest that tissue-specific miRNAs act individually or together. We propose that both cardiac and circulating miRNAs are dynamically regulated by exercise, and epigenetic mechanisms, and phenotypes are also regulated by miRNAs. A total of nine miRNAs were differentially expressed between the exercise and control groups in both tissues. miR-194-5p upregulation was quite high in heart tissue (FC=92,766) (table 5).

miRNAs exert their effects on cellular mechanisms through their target genes. The miRDBase, miRWalk, and Qiagen IPA databases were screened for target genes of miRNAs (table 6). A comparison of these three miRNAs (based on match score $\geq 80\%$) with matching scores and target genes in the miRDB database revealed that 10 genes were the common targets for miR-194-5p and miR-290. Finally, all common genes were found to be expressed in the cardiovascular system (<https://www.nextprot.org>) and CH (<https://www.disgenet.org/browser/0/1/0>) for human gene comparisons (/C1383860/25/100/source_ALL/_b./). In conclusion, we determined that the *Hand2* gene, which is the target of miR-194-5p in rats, also causes CH in humans. We also found that the *Gxylt1* gene was a common target of both miR-194-5p and miR-290, with a 93% match score (see mirDB). Although the *Socs5*, *Ube2v2*, *Acdb3*, *Elk4*, *Steap2*, *Xpnpep3*, *Neto1*, and *Tra2b* genes are targets of both miR-194-5p and miR-290, the match score for miR-194-5p is greater than 80%, while miR-290 match

Table 6. miRNAs and their target genes

| miRNA name | Target genes (miRBase, mirwalk, Qiagen IPA) | Target genes (<i>Rattus norvegicus</i>) (miRDB) | Target genes associated with CH (C1383860) (<i>Homo sapiens</i>)* |
|---------------|----------------------------------------------------------------------------------------------------------------------------------------------------------------------------------------------------------------------------------------------------------------------------------------------------------------------------------------------------------------|-------------------------------------------------------------------------------------------------------------------------------------------------------------------------------------------------------------------------------------------------------------------------------------------------------------------------------------------------------------------------------------------------------------------------------------------------------------------------------------------------------------------------------------------------------------------------------------------------------------------------------------------------------------------------------------------------------------------------------------------------------------------|----------------------------------------------------------------------------------------------------------------------------------------------------------------------------------------------------------------------------------------------------------------------------------------------------------------------------------------------------------------------------------------------------------------------------------------------------------------------|
| mo-miR-132-3p | <i>Rasa1, Pten, Mmp9^c, Mecp2, Grin2a, Capn8, Arhgap32</i> | <i>Wiz, Irx2, Senp3, Cd302, Parp14, Pcdh9, Xpo6, Gpr15, Nid2, Ppil3, Mylk, Spart, Maff, Tent4b, Dusp7, Unc13d, Spats2, Igfbp3, Txndc15, Kcns1, Meam, Pomk, Rnf148, Ppp1r7, Snap29, Cldn18, Gclc, Csdc2, Qpctl, Mmachc, Zfp217, Cd4, Clec12b, Psm11, Polr2h, Ctnd1, Zcchc7</i> | <i>MIR125B2, PLD2, POMC, PPARA, PPARD, PRKAA2, PRKCA, PRKCB, PRKCZ, PLD1, PIK3CG, SIRT6, MIR21, MT2A, MYBPC3, NOS3, NPPA, NPPB, ATP2A2, NPR1, TBX20, MFN2, REN, TRIM63</i> |
| mo-miR-194-5p | <i>Ifitm3, Rtn4, Fabp3, Ubr5, Hrt1, Cast, Human Endothelin 3, Ldhh, Prkab, Hrat13, Hrat17, Hrat5, Hrat56, Hrat92, Lbh, Hand1^c, Hand2^a, Heg1, Hras, Myo9b, Sgk223, Fabp3-ps1, Fabp3-rs2, Fabp3-rs3, Kras, Pom121L2, Rraas, Svopl, Atp1f1, Kras2-rs1, Kras2-rs2, LOC441081, LOC728488, LOC728506, Syngap1, Krasp1, Linc-rbe, Catumaxon</i> | <i>Nfat5, RGD1308601, Ube2q11, Luc7l3, Lurap1l, Fam107b, Rsb1l1, Smarca5, Hook3, Stx1b, Sgce, Zfp398, Lrrfip1, Cdk19, Bicd2, Gxylt1^b, Trim23, Socs5, Cbl1l, Lingo2, Cbln4, Ube2v2, Arhgap21, Pdlim3, Acbd3, Mid1ip1, Ptpn20, Arl6ip6, Entpd4, Fbxo33, Setd5, Nude, Myrf, Rai1, Brms1l, Cln5, Med4, Prickle2, Chd1, Tent5a, C1qtnf3, Gca, Oxt, Rabac1, Cul4b, Got2, Hspa4l, Ostm1, Nrn1, Hectd2, F13b, Slc7a5, Col4a3bp, Hnf1b, Xpo4, Col14a1, Ttc26, Pdhb, Sephs1, Bckdha, Gpat4, Ergic2, Hibadh, Slc5a7, Grhl2, Gyg1, Cln1, Ncl, Pold3, Ache, Sdc4, Exo5, Elk4, Smurf2, Luc7l, Epc2, Sumo2, Lrrc4c, Steap2, Ptpn12, Pitpnm2, Xpnpep3, Pgg1b, Cenpn, Tspan7, Neto1^b, Tmem109, Zfhx4, Tra2b, Igsf11, Lpin2, Api5, Slc35f6, Gucy1b1, Gpx8</i> | <i>CAV1, CAV3, PLPP3, CCND2, MYOCD, HAND2^a, ROCK2, UCP2, TRPC1, TNNT2, RRAD, SHC1, SLC2A4, SOD2, SOX4, SRC, STAT3, TNF, AKAP5, FHL2, GRK2, CYP2E1, DMD, AGT, EDN1, AHR, AKT1, FGF2, CYP1B1, CYP1A1, GLRX3, RBCK1, CPT1B, ADRA1B, NKX2-5f, SVOP, CTF1, ADRA2A, ADRA2C, SIRT4, CABIN1, HMOX1, HRC, HTR2B, IDH2, IGF1, IL1B, IL18, ITPR2, LIF, HIF1A, HDAC2, GSN, FNDC5, BAMBI, AOC1, GAS6, GATA4, GSK3B, AGTR1, ESRRG, FGF1, LINC02694, SPRY4-AS1, RAF1</i> |
| mo-miR-290 | <i>Vsn1l, Tagln, Syne1, Stx1a, Ssr3, Sept3, Rcan1, Ptp4a2, Ptges, Ogt, Nr4a1, Mmp9, Mgst1, Mapre1, Mapk1, Klfl5^c, Golph3, Gnb1, Gmfb, Fgf16, Delk1, Cntn4, Capn8, Arc, Akap6, Adora1, Acvr1</i> | <i>Plagl1, Nexmif, Afdn, RGD1310553, Svbp, Tm4sf1, Msl3, Btg3, Rcan2, Becn1, Spib, Pank3, CerK, Gxylt1^b, LOC257650, Col9a1, Zfp644, Chp1, Glb1, Acvr1b, Ces1d, Zkscan1, Anks1b, Kdm5a, Usp1l, Tp63, Cnot6l, Coa3, Actbl2, Sike1, Hyou1, Ccdc8, Rexo1, Tpbg, Eaf2, Rhpn2, Etv1, Srsf3, Scn7a, Sec24a, Pcmt1, Selenof, Golga1, Shroom3, Zerb1, Sox2, Erbb2, Cd40, Ddx58, Ccl2, Ppp4r3a, Ciao1, Cited2, Gpkow, Supt16h, Rps6ka2, Tnrc6b, Pik3c2a, LOC680039, Krit1, Ubxn2b, Neto1^b</i> | |

^a The *Hand2* gene is a common target in rats and humans.^b The *Neto1* gene is a common target for miR-194-5p and miR-290 in the rat.^c The *Mmp9*, *Hand1*, and *Klfl5* genes are associated with CH (Thattaliyath et al. 2002; Fan et al. 2012; Leenders et al. 2012).*<https://www.nextprot.org>, https://www.disgenet.org/browser/0/1/0/C1383860/25/100/source_ALL/_b/

Table 7. ROC curve analysis of miRNAs among the studied groups

| Compared groups | Tissue | Test variables | AUC | 95% CI | p-Value | Specificity | Sensitivity | Criterion |
|-------------------------|--------|-----------------------|-------------|--------------------|-------------------|--------------|--------------|-----------------|
| Training versus control | Heart | rno-miR-98-5p | 0.63 | [0.34–0.85] | 0.405 | 33.33 | 100 | ≤2.59 |
| | | rno-miR-106b-5p | 0.59 | [0.31–0.83] | 0.567 | 44.00 | 100 | ≤8.89 |
| | | rno-miR-132-3p | 0.72 | [0.48–0.91] | 1.469 | 77.78 | 83.33 | >0.60 |
| | | rno-miR-192-5p | 0.55 | [0.28–0.80] | 0.763 | 100 | 33.33 | >15.49 |
| | | rno-miR-194-5p | 0.94 | [0.69–0.99] | <0.0001 | 100 | 83.33 | >9.68 |
| | | rno-miR-290 | 0.92 | [0.67–0.99] | <0.0001 | 88.89 | 100 | ≤11.13 |
| | | rno-miR-350 | 0.63 | [0.34–0.85] | 0.405 | 33.33 | 100 | ≤2.59 |
| | | rno-miR-466b-2-3p | 0.72 | [0.43–0.91] | 0.152 | 66.67 | 83.33 | ≤11.63 |
| | | rno-miR-6332 | 0.72 | [0.43–0.91] | 0.150 | 66.70 | 83.00 | ≤11.72 |
| | Serum | rno-miR-98-5p | 0.73 | [0.44–0.92] | 0.086 | 44.44 | 100 | >2.44 |
| | | rno-miR-106b-5p | 0.50 | [0.23–0.76] | 1.000 | 44.44 | 83.33 | >1.80 |
| | | rno-miR-132-3p | 0.88 | [0.62–0.99] | <0.0001 | 100 | 66.67 | >0.60 |
| | | rno-miR-192-5p | 0.70 | [0.41–0.90] | 0.178 | 77.78 | 16.67 | ≤0.15 |
| | | rno-miR-194-5p | 0.60 | [0.32–0.83] | 0.000 | 100 | 33.33 | >2.65 |
| | | <i>rno-miR-290</i> | 0.50 | [0.24–0.76] | 0.954 | 55.56 | 16.67 | >0.79 |
| | | rno-miR-350 | 0.68 | [0.40–0.89] | 0.212 | 55.56 | 83.33 | >3.87 |
| | | rno-miR-466b-2-3p | 0.70 | [0.41–0.90] | 0.251 | 88.89 | 66.67 | >–2.47 |
| | | rno-miR-6332 | 0.52 | [0.26–0.78] | 0.877 | 100 | 33.33 | >–0.83 |

AUC, area under the curve; CI, confidence interval.

Boldface shows miRNAs whose activities change.

score is below 80% (table 6) (matching score data from databases and matching scores of 80 and above are given for target specificity).

3.4 ROC analysis of miRNAs

In heart tissue, the AUC value was calculated as 0.944 (95% CI=0.696–0.999, $p=0.0001$) for rno-miR-194-5p and as 0.926 (95% CI=0.670–0.997, $p=0.0001$) for rno-miR-290. In addition, the AUC value for rno-miR-132-5p in serum was calculated as 0.889 (95% CI=0.623–0.990, $p=0.0001$) (table 7). AUC of other miRNAs (rno-miR-98-5p, rno-miR-106b-5p, rno-miR-192-5p, rno-miR-350, rno-miR-466b-2-3p, and rno-miR-6332) are in table 7 and figure 3. The ROC analysis revealed that three miRNAs could be potential biomarkers. There was no correlation between miRNAs and other parameters (exercise, echocardiography, and tissue analysis) ($p>0.05$). Based on the results of this study, the expression levels of the three miRNAs make them potential biomarker candidates of the CH. Consequently, miRNAs expressed in serum and heart tissues are differentially expressed in exercise-induced CH. In the ROC analysis model, when all miRNAs expressed in the heart tissue and serum were taken together (DeLong *et al.* 1988), different miRNA pair combinations were significant (table 8).

3.5 Histological analysis of cardiac tissue

According to the results of HE and Masson Trichrome staining, heart tissue sections belonging to the CG had a histologically normal appearance. In the CG, cardiomyocytes were distributed evenly and regularly (HE). The connective tissue had normal appearance, and there was no fibrosis in the CG (Masson Trichrome) (figure 4a and b). In the TG, hyperchromatic nuclei, enlarged cytoplasm, and myocyte disarray with moderate myocyte hypertrophy were observed (HE). Myocyte disarray with mild interstitial fibrosis (<5%) was observed in the TG (figure 4c and d). According to the pathological scoring, myofibrillary dysregulation ($p=0.043$) and interstitial fibrosis ($p=0.005$) were found to be significant in the TG, but there was no correlation with cardiomyocyte hypertrophy ($p>0.05$) (Masson Trichrome). We observed that the healthy cells in the TG stained pale with Masson Trichrome, in contrast to the cells undergoing necrosis. Intensive areas of bleeding and edema were found between the heart muscle fibers. Heart muscle fibers diverged from each other due to edema and bleeding. Also, congestion was found in some of the sections. The average histopathologic scoring was calculated as 2.50 ± 1.87 for the CG and 7.44 ± 1.51 for the TG ($p=0.03$).

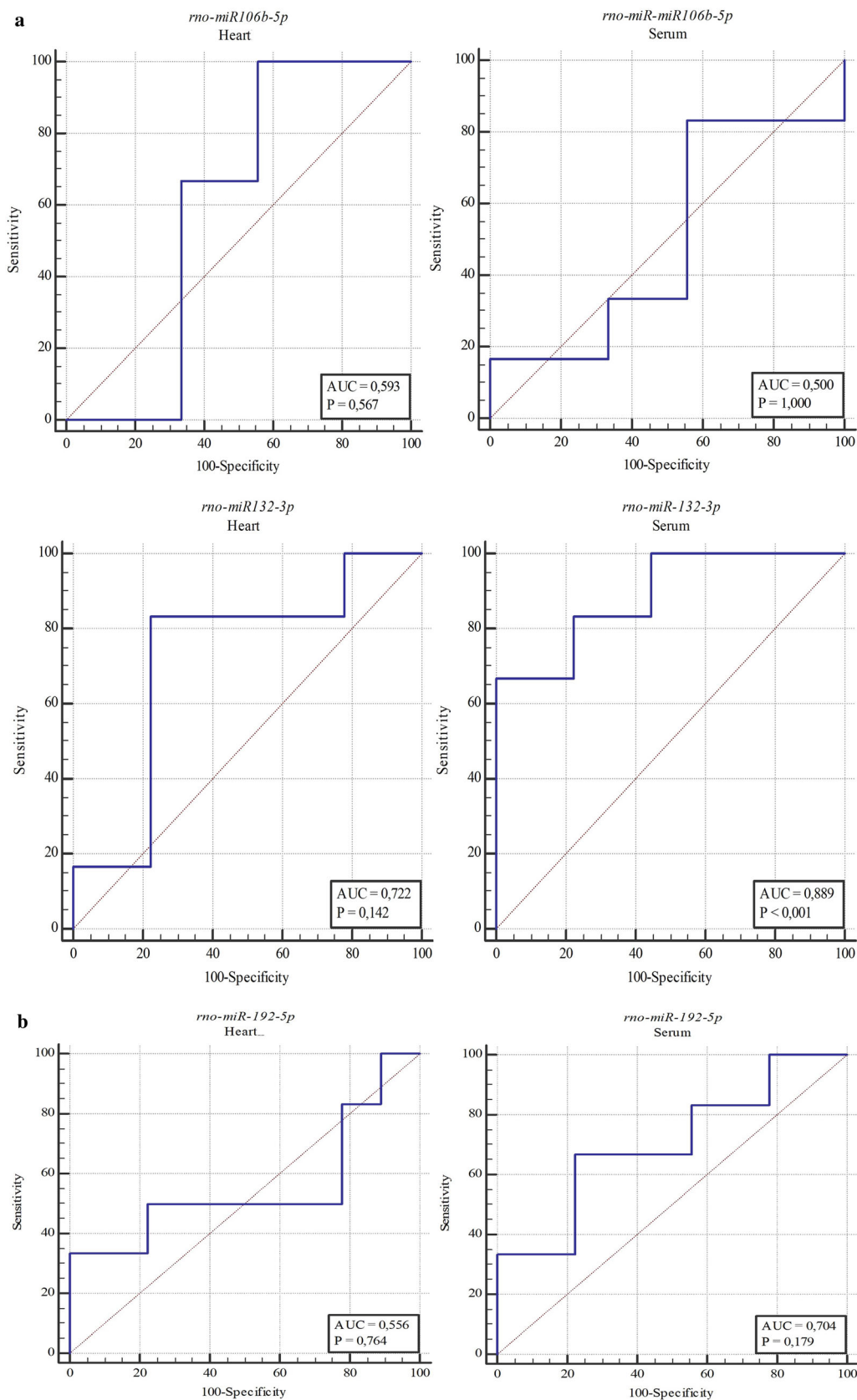


Figure 3. ROC analysis of miRNAs.

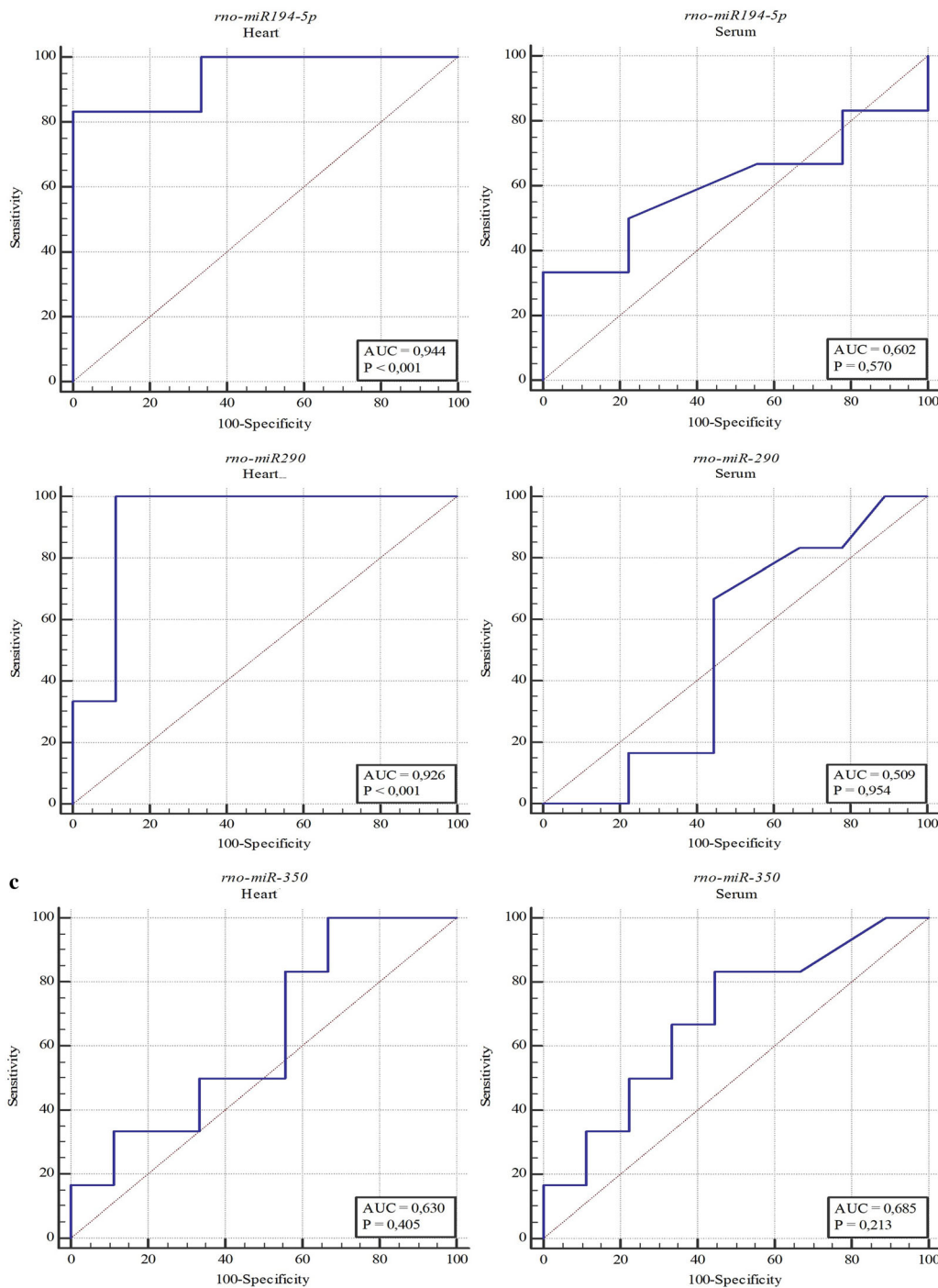


Figure 3. (continued.)

3.6 Apoptotic cardiomyocytes detection by TUNEL

The placement of fibrous connective tissue after the loss of cardiomyocytes due to apoptosis is the most important feature of cardiac remodeling. As a result

of TUNEL staining performed to show apoptosis, positive cells were rarely found in CG and TG. An average of 6–7 cells per section in each group was detected. Therefore, it is thought that exercise does not cause cell death by apoptosis (figure 5) ($p > 0.05$).

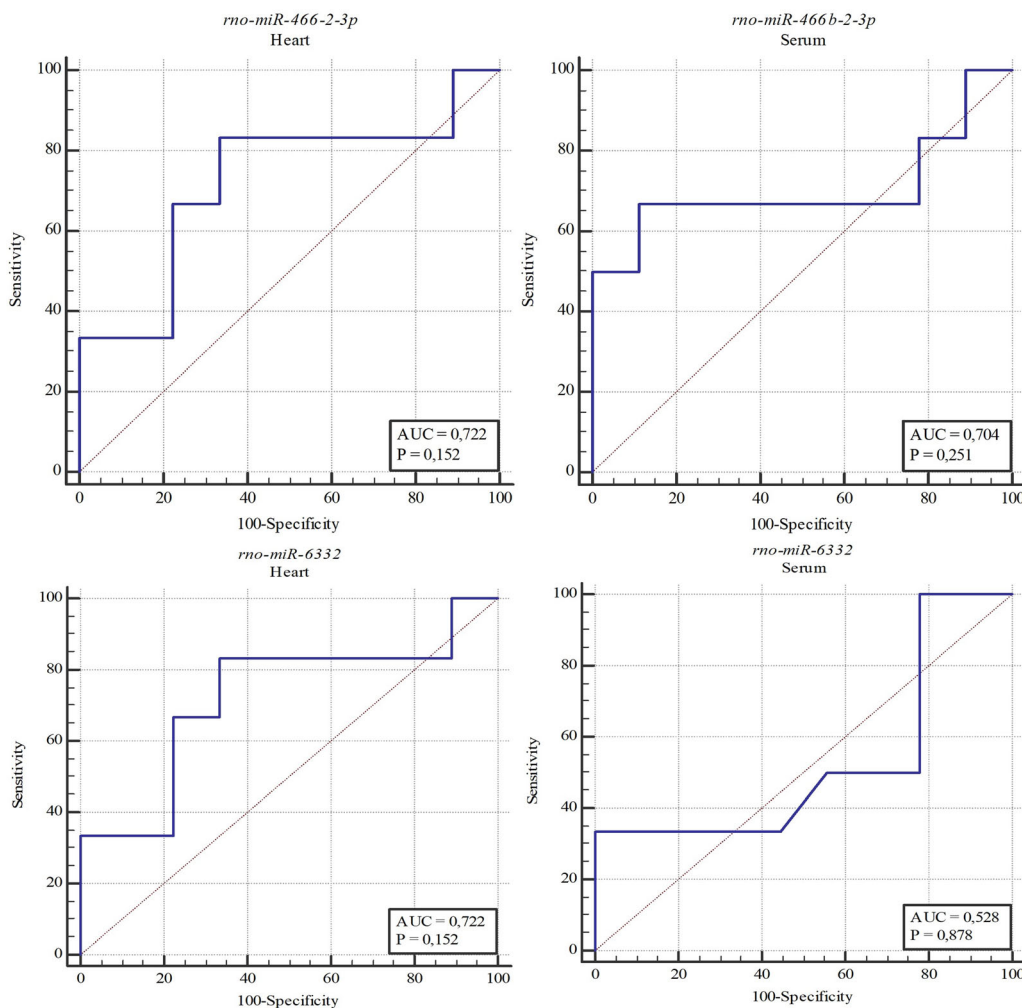


Figure 3. (continued.)

3.7 Proliferation of cardiomyocytes with immunohistochemistry

The necessary response to the increase in biomechanical stress is given by expanding myofibrils in the heart. Although hypertrophy returns the wall tension to normal, its negativity causes heart failure or sudden death in affected individuals. In the histological analysis for the evaluation of cell proliferation, no PCNA-positive cells were found in the cardiomyocytes of both control and exercise groups. Although it is known that miRNAs have a potential effect on the regulation of cardiomyocyte proliferation, it was determined in this study that miRNAs do not have a direct role in the regulation of active proliferation required for cardiac remodeling. Therefore, it was concluded that exercise did not cause proliferation in cardiomyocytes ($p > 0.05$) (figure 6).

4. Discussion

miRNAs positively or negatively regulate the hypertrophic growth response of the heart, depending on the stress. Therefore, identifying the pathways in which miRNAs are involved is extremely important to understand the mechanism of CH. On the other hand, miRNAs exert effects through their target genes. Identification of target genes is significant for demonstrating pathways in CH. miRNAs have functions in cardiomyocyte growth, remodeling, and processes such as vascularization.

CH is the increased size of the cardiomyocyte resulting from prolonged stress and volumetric stretching of the heart (Müller and Dhalla 2013). Exercise, hypertension, or other pathologies may cause hypertrophy (Johnson *et al.* 2015). In CH, various changes occur in the growing myocytes, from gene

Table 8. Full model of ROC analysis for all miRNA in heart tissue and serum

| miRNA pair | Tissue | Difference between areas | Standard error | 95% CI | z-Statistic | p-Value |
|----------------------------------------|--------|--------------------------|----------------|----------------|-------------|--------------|
| rno-miR-98-5p ~ rno-miR-106b-5p | Heart | 0.037 | 0.156 | [-0.268–0.342] | 0.238 | 0.812 |
| rno-miR-98-5p ~ rno-miR-132-3p | | 0.092 | 0.169 | [-0.239–0.424] | 0.547 | 0.584 |
| rno-miR-98-5p ~ rno-miR-192-5p | | 0.074 | 0.206 | [-0.329–0.477] | 0.360 | 0.718 |
| rno-miR-98-5p ~ rno-miR-194-5p | | 0.315 | 0.161 | [-0.001–0.631] | 1.951 | 0.051 |
| rno-miR-98-5p ~ rno-miR-290 | | 0.296 | 0.145 | [0.011–0.581] | 2.037 | 0.041 |
| rno-miR-98-5p ~ rno-miR-350 | | 0.000 | 2.634 | [-5.162–5.162] | 0.000 | 1.000 |
| rno-miR-98-5p ~ rno-miR-466b-2-3p | | 0.092 | 0.188 | [-0.276–0.461] | 0.492 | 0.622 |
| rno-miR-98-5p ~ rno-miR-6332 | | 0.090 | 0.179 | [-0.280–0.468] | 0.500 | 0.630 |
| rno-miR-106b-5p ~ rno-miR-132-3p | | 0.130 | 0.130 | [-0.612–0.384] | 1.001 | 0.317 |
| rno-miR-106b-5p ~ rno-miR-192-5p | | 0.037 | 0.239 | [-0.431–0.505] | 0.155 | 0.876 |
| rno-miR-106b-5p ~ rno-miR-194-3p | | 0.352 | 0.181 | [-0.002–0.706] | 1.945 | 0.051 |
| rno-miR-106b-5p ~ rno-miR-290 | | 0.333 | 0.142 | [0.050–0.612] | 2.347 | 0.018 |
| rno-miR-106b-5p ~ rno-miR-350 | | 0.037 | 0.156 | [-0.268–0.342] | 0.238 | 0.812 |
| rno-miR-106b-5p ~ rno-miR-466b-2-3p | | 0.130 | 0.139 | [-0.143–0.402] | 0.933 | 0.350 |
| rno-miR-106b-5p ~ rno-miR-6332 | | 0.128 | 0.141 | [-0.152–0.410] | 0.938 | 0.346 |
| rno-miR-132-3p ~ rno-miR-192-5p | | 0.167 | 0.213 | [-0.252–0.585] | 0.781 | 0.435 |
| rno-miR-132-3p ~ rno-miR-194-5p | | 0.222 | 0.188 | [-0.146–0.590] | 1.184 | 0.236 |
| rno-miR-132-3p ~ rno-miR-290 | | 0.204 | 0.127 | [-0.045–0.453] | 1.602 | 0.109 |
| rno-miR-132-3p ~ rno-miR-350 | | 0.092 | 0.169 | [-0.239–0.424] | 0.547 | 0.548 |
| rno-miR-132-3p ~ rno-miR-466b-2-3p | | 0.000 | 0.157 | [-0.307–0.307] | 0.000 | 1.000 |
| rno-miR-132-3p ~ rno-miR-6332 | | 0.000 | 0.161 | [-0.298–0.310] | 0.000 | 1.000 |
| rno-miR-192-5p ~ rno-miR-194-5p | | 0.389 | 0.182 | [0.030–0.745] | 2.142 | 0.032 |
| rno-miR-192-5p ~ rno-miR-290 | | 0.037 | 0.200 | [-0.021–0.763] | 1.851 | 0.064 |
| rno-miR-192-5p ~ rno-miR-350 | | 0.074 | 0.206 | [-0.329–0.477] | 0.360 | 0.718 |
| rno-miR-192-5p ~ rno-miR-466b-2-3p | | 0.167 | 0.208 | [-0.241–0.575] | 0.800 | 0.423 |
| rno-miR-192-5p ~ rno-miR-6332 | | 0.170 | 0.205 | [-0.250–0.568] | 0.798 | 0.430 |
| rno-miR-194-5p ~ rno-miR-290 | | 0.018 | 0.112 | [-0.201–0.238] | 0.165 | 0.868 |
| rno-miR-194-5p ~ rno-miR-350 | | 0.315 | 0.161 | [-0.001–0.631] | 1.951 | 0.051 |
| rno-miR-194-5p ~ rno-miR-466b-2-3p | | 0.222 | 0.189 | [-0.148–0.592] | 1.177 | 0.239 |
| rno-miR-194-5p ~ rno-miR6332 | | 0.220 | 0.192 | [-0.154–0.600] | 1.176 | 0.242 |
| rno-miR-290 ~ rno-miR-350 | | 0.296 | 0.145 | [0.012–0.581] | 2.037 | 0.041 |
| rno-miR-290 ~ rno-miR-466b-2-3p | | 0.204 | 0.137 | [-0.065–0.472] | 1.486 | 0.137 |
| rno-miR-290 ~ rno-miR-6332 | | 0.208 | 0.146 | [-0.072–0.451] | 1.475 | 0.145 |
| rno-miR-350 ~ rno-miR-466b-2-3p | 0.096 | 0.188 | [-0.276–0.461] | 0.492 | 0.622 | |
| rno-miR-350 ~ rno-miR-6332 | 0.089 | 0.176 | [-0.284–0.470] | 0.486 | 0.631 | |
| rno-miR-466b-2-3p ~ rno-miR6332 | 0.000 | 2.634 | [-5.162–5.162] | 0.000 | 1.000 | |
| rno-miR-98-5p ~ rno-miR-106b-5p | Serum | 0.231 | 0.238 | [-0.235–0.698] | 0.973 | 0.336 |
| rno-miR-98-5p ~ rno-miR-132-3p | | 0.157 | 0.115 | [-0.067–0.382] | 1.372 | 0.170 |
| rno-miR-98-5p ~ rno-miR-192-5p | | 0.027 | 0.234 | [-0.431–0.486] | 0.119 | 0.905 |
| rno-miR-98-5p ~ rno-miR-194-5p | | 0.130 | 0.244 | [-0.348–0.607] | 0.532 | 0.594 |
| rno-miR-98-5p ~ rno-miR-290 | | 0.222 | 0.241 | [-0.250–0.694] | 0.922 | 0.356 |

Boldface indicates *p*-value less than 0.05.

expression to hormone levels (Dillmann 2010). These changes can cause heart failure. miRNAs are involved in normal and pathological processes of biological systems (Condrat *et al.* 2020). In this study, we investigated the relationship between the expression behavior of miRNAs in the cardiac tissue and serum, and changes at the structural and tissue levels of the heart in a swimming exercise-induced CH model in rats.

Studies show that miRNAs are physiologically involved in cardiac remodeling induced by exercises such as swimming and running (Wang *et al.* 2018). Soci *et al.* (2011) investigated the functions of miRNAs in CH induced by aerobic exercise in rats. Researchers used two different exercise programs. The first program was low-intensity, long-term; and the second program consisted of a low-intensity and longer-term exercise program. The aim of the researchers was first to

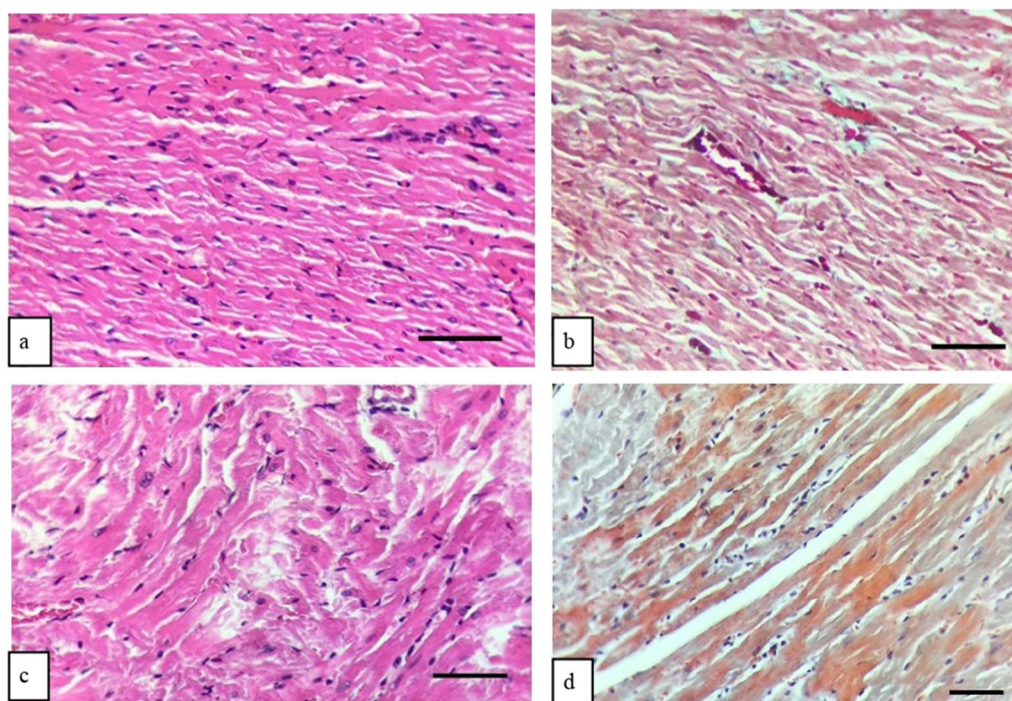


Figure 4. Heart tissue sections belonging to the CG: Normal histological appearance (a) Hematoxylin & Eosin, $\times 40$. (b) Masson Trichrome staining, $\times 40$ (scale bar: 50 μm). Heart tissue sections belonging to the TG: (c) Myocyte disarray with hypertrophy of myocytes in sample 9 (Hematoxylin & Eosin, $\times 40$). (d) Myocyte disarray with mild interstitial fibrosis in sample 9 (Masson Trichrome, $\times 40$) (scale bar: 50 μm).

stimulate cardiovascular adaptations and increase the oxidative capacity of the muscles. The second aim of the study was that the exercise duration increased, and there was an increase in the heart rate and aerobic performance. After completing the exercise protocol, systolic and diastolic functions of the heart were evaluated with echocardiography. There was no difference in systolic function between the exercise and control groups, and ventricular compliance improved in the exercise group. In our study, the first monitoring indicators of hypertrophic development were the echocardiographic measurements performed before and after the exercise program. After the swimming exercise program, left ventricular mass, left ventricular end-diastolic diameter, left ventricular end-systolic diameter, posterior wall thickness, and interventricular septum thickness of the TG increased significantly compared with the baseline values in the ECHO examination (table 1). We also showed hypertrophy histologically (figure 5). The development of LV hypertrophy is a response to pressure overload and is a desirable outcome in this study.

Permanent hypertrophy due to increased load after exercise is a risk factor for sudden cardiac death (Kokubo *et al.* 2005). To prevent this type of

hypertrophy, it is significant to clarify the underlying mechanisms. In this study, we propose that swimming exercise-induced CH is regulated by miRNAs via matrix metalloproteinases (Doxakis *et al.* 2019) and HAND basic Helix-Loop-Helix (bHLH) transcription factors (Thattaliyath *et al.* 2002). These *HAND* genes are possible target genes of miRNAs. Cardiac remodeling process is regulated negatively or positively by miRNAs. It is reported that heart-specific miRNAs affect cardiac parameters during cardiac remodeling (Topkara and Mann 2010).

In this study, the expression levels of heart tissue-specific miRNAs (based on data in databases) were low in the normal tissue. According to our results, rno-miR-194-5p was upregulated while rno-miR-290 was downregulated in the heart tissue of the exercise group. On the other hand, rno-miR-132-3p was upregulated in the serum of the exercise group. Because the miRNAs have tissue-specific expression, they may behave differently. In this study, the relationship of these miRNAs, whose expression we detected changes, with CH is shown for the first time (to the best of the authors' knowledge).

Maron showed that V_{mass} , $LVDd$, $LVDs$, and $LPWT$ of athletes increased compared with the CG

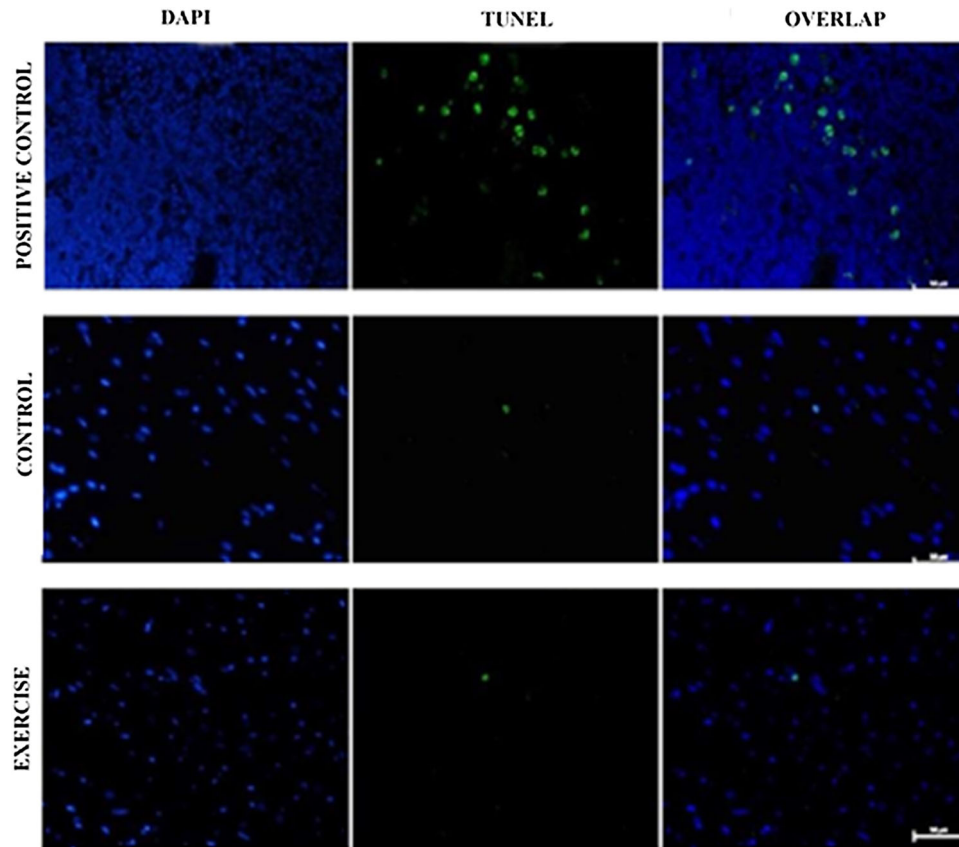


Figure 5. Appearance of apoptotic cells in cardiac myocytes using TUNEL fluorescent staining technique. All cells are in blue color, and TUNEL positive cells are in green color.

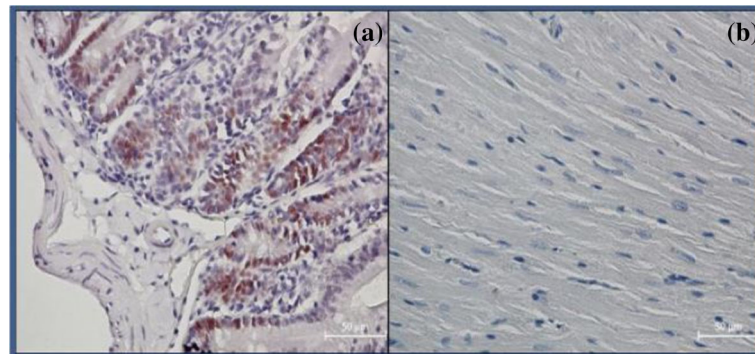


Figure 6. Training and cardiomyocyte proliferation. Light microscopic view of PCNA-positive cells (magnification: 40 \times). (a) PCNA-positive cells (dark brown) in the mouse intestine section considered as positive control. (b) No PCNA-positive cells were found in cardiac myocytes belonging to the TG.

(Maron 1986). In this study, the decrease in % LVEF of the exercise group compared with the CG is consistent with the results of Fernandes *et al.* (2011). There are various studies on the LVEF value showing systolic function in athletes. In one of these studies, Maron (1986) reported that LVEF was within normal limits in most of the athletes (Maron 1986). Rerych *et al.* (1980) showed decreased LVEF in swimmers, while Stein

et al. (1980) showed that LVEF slightly increased after exercise. In our study, the % LVEF value of the TG decreased significantly after the exercise program which is consistent with the results of Rerych *et al.* (1980).

In this study, cell proliferation was evaluated to demonstrate the development of CH. There was no significant proliferation in CG and TG. CH causes an

increase in the area and width of cardiomyocytes without any change in the number of cardiomyocytes. It is known that there is a proliferation in 1% of cardiomyocytes in the adult heart (Batista and Chang 2013). As a result, we think that our analysis results of histological examinations evaluating proliferation are compatible with the literature.

Many studies have shown a relationship between miRNAs and CH. Fernandes *et al.* (2011) demonstrated the expression of 349 different miRNAs by microarray method in the heart tissues of rats when they applied two alternative swimming exercises. Among the differentially expressed miRNAs, six miRNAs (miR-1, -133a, -133b, -29a, -29b, and -29c) were selected. It has been shown in previous studies that these six genes are involved in CH caused by pathological stress (Care *et al.* 2007; van Rooij *et al.* 2008a, b). It is stated that changes in the expression of these miRNAs are involved in pathological hypertrophy (van Rooij *et al.* 2008a, b).

In this study, 25,000 genes in the rat genome were screened by the microarray method. There was a change in the expression of 128 miRNAs. Of these 128 miRNAs, 119 were upregulated and nine were downregulated. Nine of these miRNAs were selected, and the expressions of these nine genes were confirmed by the RT-PCR method.

In this study, for the first time, we detected the change in expression of these three miRNAs (miR-290, miR-194-5p, and miR-132-3p) in swimming-induced physiological CH. Among the targets of these miRNAs, we identified in our study the Kruppel-like factor 15 (Klf15) as the target of miR-290 that causes physiological CH. Klf15 was identified as an inhibitor of CH (Fisch *et al.* 2007) and was overexpressed in cardiomyocytes of newborn rats. This overexpression inhibits cell growth, protein synthesis, and hypertrophic gene expression (Patel *et al.* 2018). Klf15 is a transcription factor found in the nucleus and is involved in various biological processes such as proliferation, differentiation, growth, development, and response to external stress (McConnell and Yang 2010). *KLF15*-null mice have been shown to develop fibrosis and store excess collagen in their hearts (Wang *et al.* 2008). These studies show that *KLF15* plays a role in the pathogenesis of fibrotic diseases in the heart by causing an increase in the expression of connective tissue growth factor (CTGF). Overexpression of Klf15 suppresses basal and TGF- β 1-induced CTGF expression. These studies suggest that Klf15 negatively regulates cardiac fibrosis. Klf15 can prevent cardiac fibrosis by transcriptionally inhibiting CTGF

expression. Klf15 constitutes CH by causing inhibition of the calcineurin-NFAT signaling pathway in cardiomyocytes. We can say that miR-290 is involved in the calcineurin-NFAT signaling pathway through its target gene, *KLF15*.

The targets of miR-194-5p are the Hand genes which are a subclass of bHLH transcription factors and consist of two genes (*Hand1* and *Hand2*). The *Hand1* and *Hand2* genes are involved in the normal development of the heart and extra-embryonic development in fish, rodents, and humans. The *Hand1* and *Hand2* genes are expressed in both ventricles and are downregulated in CH (Natarajan *et al.* 2001). One study reported that downregulation of *Hand* genes leads to CH and later to cardiomyopathy (Thattaliyath *et al.* 2002). The *Hand1* and *Hand2* genes are involved in the signaling pathway of nuclear factor-activated T cells (NFAT). NFAT plays a significant role in the activation of the hypertrophic gene program. In response to hypertrophic stimulation, NFAT is dephosphorylated by calcineurin. NFAT activates gene expression in the nucleus. The *Hand1* and *Hand2* genes are among the genes that are activated. In addition, the *Hand2* gene prevents cardiac muscle cells from undergoing apoptosis. In this mechanism, activation of miR-194-5p is responsible for directing cells to necrosis rather than apoptosis (Bernardo *et al.* 2010). This result is consistent with our histological results. The change in miR-194-5p expression in necrotic heart tissue regulates the production of cytokines involved in inflammation (Moschos *et al.* 2007). The expression of miR-194-5p is significant in both formations of hypertrophy and the elimination of the harmful effects of inflammation.

In this study, cardiac muscle cells preserved their histological features in the CG, and there were no pathological findings. Moderate myocyte hypertrophy, mild interstitial fibrosis, necrosis, hemorrhage, intercellular edema, and myocyte irregularity were detected in the TG (figure 5). The mean histopathological score in the TG was significantly higher than in the CG. Our results showed that prolonged exercise did not cause cell death via apoptosis, and cells went into necrosis. In a study in patients with acute myocardial failure, elevated serum levels of three miRNAs, including miR-194, were observed. In this study, heart failure developed in patients within one year. miR-194 has been reported to be released directly from necrotic heart tissue into the blood and has a short half-life (Baggish *et al.* 2014). In another study, the functions of miRNAs have been investigated in a model of inflammation created using lipopolysaccharide in a mouse liver. The expressions of 12 miRNAs, including miR-194, are

increased (Moschos *et al.* 2007). Sayed *et al.* (2007) investigated miRNAs by microarray method in a mouse CH model induced by transverse aortic constriction due to excessive pressure. According to the analysis results obtained by taking the heart tissue of mice 1, 7, and 14 days after the operation; it was observed that miR-290 was downregulated on the first three days, upregulated on the 4th, 5th, and 6th days, downregulated on the 7th and 8th days, and there was no change in its expression on the 9th day. miR-194 saw no change in its expression on the 1st and 6th days, was downregulated on the 7th day, not expressed on the 8th day, and downregulated on the 9th day (Sayed *et al.* 2007). The differences seen in the expression of miR-194 and miR-290 depend on how CH is formed. However, as we have shown in our study, it is a fact that they are abnormal miRNAs in the process of cardiac hypertrophy and contribute to the cardiac remodeling process.

One study on miR-132 analyzed 106 circulating inflammatory miRNAs from blood samples from nine active middle-aged men before and after marathon running. There was an increase in the level of 12 inflammatory miRNAs that cause inflammation after the marathon run. One of the increased miRNAs is miR-132-3p (de Gonzalo-Calvo *et al.* 2015). In another study, it is stated that miR-132 functions in the nervous and cardiovascular systems. Psychic stress causes a decrease in brain-derived neurotrophic factor (BDNF) levels. It causes a decrease in CREB activation and miR-132 to be downregulated. This causes deterioration of neuroplasticity and depression. Stress also leads to a decrease in miR-132 through the increase in glucocorticoids. Besides, miR-132 affects cardiovascular function through the autonomic nervous system and the hypothalamus–pituitary–adrenal gland (HPA axis). Most of the circulating BDNF is produced in the brain, and can cross the blood–brain barrier and affect cardiovascular function, including miR-132 expression level. The level of miR-132 produced in the brain is related to the level found in the cardiovascular system. It is emphasized that miR-132 should be upregulated in the treatment of depression and cardiovascular diseases (Zheng *et al.* 2013).

Studies have stated that five miRNAs (miR-29b, -129-3p, -132, -132, and -212) identified in cultured cells and adult cardiac fibroblasts are associated with cardiovascular diseases such as hypertrophy, myocardial infarction, and fibrosis. These miRNAs activate the signaling pathway dependent on G α q/11 and cause maladaptive hypertrophy, which leads to fibrosis (Jeppesen *et al.* 2011).

In this study, it was shown for the first time that the circulating expression of miR-132-3p was 16.6 fold in the cardiac hypertrophy model created by swimming exercise. The target gene of miR-132-3p, which was experimentally validated using miRWalk and miRTarBase, was determined to be Matrix Metalloproteinase 9 (MMP9). Collagen is at a normal level with the decrease of MMP9 in the healthy heart, and heart health is protected by causing the differentiation of cardiac stem cells. Increased expression of MMP-9 causes an increase in collagen levels. This, in turn, inhibits the differentiation of cardiac stem cells, leading to the pathological cardiac remodeling process.

As demonstrated in this study, miR-132-3p upregulation can affect the activity of MMP-9, preserving the amount of collagen in the extracellular matrix and preventing fibrosis. Upregulation of miR-132 results in the development of pathological cardiac remodeling in transgenic mice (Ucar *et al.* 2012). But, hypertrophy can be induced by overexpressing the calcineurin/NFAT pro-hypertrophic pathway by overexpressing miR-132-3p. As a result, we think that downregulated miR-290 but upregulated miR-132-3p may prevent cardiac fibrosis. Also, the significant increase in the expression of the *miR-194-5p* gene may be effective in the orientation process of the heart towards pathological hypertrophy. Also, we anticipate that the increase in the amount of miR-132-3p in the blood can be used as a marker to help identify cardiac fibrosis. Hypertrophy can also be induced by overexpressing the calcineurin/NFAT pro-hypertrophic pathway by overexpressing miR-132-3p.

In summary, this study analyzed differentially expressed miRNAs in a rat model of cardiac hypertrophy induced by swimming exercise. A total of six upregulated and three downregulated miRNAs were detected in the cardiac tissue. And three upregulated and six downregulated miRNAs were detected in serum samples of rats with cardiac hypertrophy. We demonstrated tissue-specific and circulating behavior of other investigated miRNAs, apart from miRNAs validated in the cardiac hypertrophy model with qRT-PCR. Also, we tested the sensitivity and specificity of nine miRNAs by ROC analysis. These results indicated that one miRNA could not only be a potential novel biomarker for early detection of hypertrophy but also three miRNAs could play a role in the pathogenesis of cardiac hypertrophy. Therefore, additional studies with healthy volunteers and patient groups are needed to be able to use miR-194-5p, miR-290, and miR-132-3p as biomarkers and treatment targets in human hypertrophic cardiomyopathy.

5. Conclusion

When miRNA expressions are investigated in CH, limiting factors such as the lack of standard protocols, a small number of subjects, and dynamic differences between groups emerge. In addition, fibroblasts and endothelial and inflammatory cells may contribute to cardiac processes. This study has been specified with cardiomyocytes, fibrous tissue, and serum to determine the behavior of miRNA expressions.

Loss-of-function and gain-of-function studies are used to determine the activities of miRNAs. Laboratory conditions determine the selection of these methods. miRNA-based drugs are developed that can adjust the level of target genes. The relevant miRNA needs to be expressed only in the heart. Thus, miRNAs will only be able to interact with their target genes. It may come to the fore to examine the genes that pass all stages in athlete and patient groups.

Funding

This work was supported by the Scientific Research Projects Unit of Istanbul University (Project No.: 48783).

Declarations

Conflict of interest Authors declare no conflict of interest.

Ethical standards All applicable international, national, and/or institutional principles for the care and use of animals have been observed.

References

- Artzi S, Kiezun A and Shomron N 2008 Mirnaminer: a tool for homologous microrna gene search. *BMC Bioinform.* **9** 39
- Baggish AL, Park J, Min PK, et al. 2014 Rapid upregulation and clearance of distinct circulating microRNAs after prolonged aerobic exercise. *J. Appl. Physiol.* **116** 522–531
- Barbas CF 3rd, Burton DR, Scott JK, et al. 2007 Quantitation of DNA and RNA. *Cold Spring Harb. Protoc.* <https://doi.org/10.1101/pdb.ip47>
- Barber JL, Zellars KN, Barringhaus KG, et al. 2019 The effects of regular exercise on circulating cardiovascular-related microRNAs. *Sci. Rep.* **9** 7527
- Batista PJ and Chang HY 2013 Long noncoding RNAs: cellular address codes in development and disease. *Cell* **152** 1298–1307
- Bernardo BC, Weeks KL, Pretorius L, et al. 2010 Molecular distinction between physiological and pathological cardiac hypertrophy: experimental findings and therapeutic strategies. *Pharmacol. Ther.* **128** 191–227
- Care A, Catalucci D, Felicetti F, et al. 2007 MicroRNA-133 controls cardiac hypertrophy. *Nat. Med.* **13** 613–618
- Chen C, Ponnusamy M, Liu C, et al. 2017 MicroRNA as a therapeutic target in cardiac remodeling. *BioMed. Res. Int.* **2017** 1278436
- Chen Y and Wang X 2020 miRDB: an online database for prediction of functional microRNA targets. *Nucleic Acids Res.* **48** D127–D131
- Condrat CE, Thompson DC, Barbu MG, et al. 2020 MiRNAs as biomarkers in disease: latest findings regarding their role in diagnosis and prognosis. *Cells* **9** 276
- Cunningham KS, Spears DA and Care M 2019 Evaluation of cardiac hypertrophy in the setting of sudden cardiac death. *Forensic Sci. Res.* **4** 223–240
- de Gonzalo-Calvo D, Dávalos A, Montero A, et al. 2015 Circulating inflammatory miRNA signature in response to different doses of aerobic exercise. *J. Appl. Physiol.* **119** 124–134
- DeLong ER, DeLong DM and Clarke-Pearson DL 1988 Comparing the areas under two or more correlated receiver operating characteristic curves: a nonparametric approach. *Biometrics* **44** 837–845
- de Simone G, Wallerson DC, Volpe M, et al. 1990 Echocardiographic measurement of left ventricular mass and volume in normotensive and hypertensive rats: necropsy validation. *Am. J. Hypertens.* **3** 688–696
- Dillmann W 2010 Cardiac hypertrophy and thyroid hormone signaling. *Heart Fail. Rev.* **15** 125–132
- Doxakis A, Polyanthi K, Androniki T, et al. 2019 Targeting metalloproteinases in cardiac remodeling. *J. Cardiovasc. Med. Cardiol.* **6** 51–60
- Evangelista F, Brum P and Krieger J 2003 Duration-controlled swimming exercise training induces cardiac hypertrophy in mice. *Braz. J. Med. Biol. Res.* **36** 1751–1759
- Fan D, Takawale A, Lee J, et al. 2012 Cardiac fibroblasts, fibrosis and extracellular matrix remodeling in heart disease. *Fibrogenesis Tissue Repair* **5** 15
- Fernandes T, Hashimoto NY, Magalhães FC, et al. 2011 Aerobic exercise training-induced left ventricular hypertrophy involves regulatory microRNAs, decreased angiotensin-converting enzyme-angiotensin ii, and synergistic regulation of angiotensin-converting enzyme 2-angiotensin (1–7). *Hypertension* **58** 182–189
- Fisch S, Gray S, Heymans S, et al. 2007 Kruppel-like factor 15 is a regulator of cardiomyocyte hypertrophy. *Proc. Natl. Acad. Sci. USA* **104** 7074–7079
- Helgerud J, Høydal K, Wang E, et al. 2007 Aerobic high-intensity intervals improve V O₂max more than moderate training. *Med. Sci. Sports Exerc.* **39** 665–671

- Hughes DC, Ellefsen S and Baar K 2018 Adaptations to endurance and strength training. *Cold Spring Harb. Perspect. Med.* **8** a029769
- Jeppesen PL, Christensen GL, Schneider M, *et al.* 2011 Angiotensin II type 1 receptor signalling regulates microRNA differentially in cardiac fibroblasts and myocytes. *Brit. J. Pharmacol.* **164** 394–404
- Johnson EJ, Dieter BP and Marsh SA 2015 Evidence for distinct effects of exercise in different cardiac hypertrophic disorders. *Life Sci.* **123** 100–106
- Kawahara Y, Tanonaka K, Daicho T, *et al.* 2005 Preferable anesthetic conditions for echocardiographic determination of murine cardiac function. *J. Pharmacol. Sci.* **99** 95–104
- Kiernan JA 1999 Histological and histochemical methods: theory and practice. *Shock* **12** 479
- Kokubo M, Uemura A and Matsubara T 2005 Noninvasive evaluation of the time course of change in cardiac function in spontaneously hypertensive rats by echocardiography. *Hypertens. Res.* **28** 601–609
- Krämer A, Green J, Pollard J Jr, *et al.* 2014 Causal analysis approaches in ingenuity pathway analysis. *Bioinformatics* **30** 523–530
- Leenders JJ, Wijnen WJ, van der Made I, *et al.* 2012 Repression of cardiac hypertrophy by KLF15: underlying mechanisms and therapeutic implications. *PLoS One* **7** e36754
- Liu W and Wang X 2019 Prediction of functional microRNA targets by integrative modeling of microRNA binding and target expression data. *Genome Biol.* **20** 18
- Livak KJ and Schmittgen TD 2001 Analysis of relative gene expression data using real-time quantitative PCR and the $2(-\Delta\Delta CT)$ method. *Methods* **25** 402–408
- Maron BJ 1986 Structural features of the athlete heart as defined by echocardiography. *J. Am. Coll. Cardiol.* **7** 190–203
- Maron BJ, Wolfson JK and Roberts WC 1992 Relation between extent of cardiac muscle cell disorganization and left ventricular wall thickness in hypertrophic cardiomyopathy. *Am. J. Cardiol.* **70** 785–790
- Masè M, Grasso M, Avogaro L, *et al.* 2017 Selection of reference genes is critical for miRNA expression analysis in human cardiac tissue. A focus on atrial fibrillation. *Sci. Rep.* **7** 41127
- McConnell BB and Yang VW 2010 Mammalian Krüppel-like factors in health and diseases. *Physiol. Rev.* **90** 1337–1381
- Mega C, Vala H, Rodrigues-Santos P, *et al.* 2014 Sitagliptin prevents aggravation of endocrine and exocrine pancreatic damage in the Zucker diabetic fatty rat-focus on amelioration of metabolic profile and tissue cytoprotective properties. *Diabetol. Metab. Syndr.* **6** 42
- Mokhtari B, Badalzadeh R, Alihemmati A, *et al.* 2015 Phosphorylation of GSK-3 β and reduction of apoptosis as targets of troxerutin effect on reperfusion injury of diabetic myocardium. *Eur. J. Pharmacol.* **765** 316–321
- Moschos SA, Williams AE, Perry MM, *et al.* 2007 Expression profiling in vivo demonstrates rapid changes in lung microRNA levels following lipopolysaccharide-induced inflammation but not in the anti-inflammatory action of glucocorticoids. *BMC Genomics* **8** 240
- Müller AL and Dhalla NS 2013 Differences in concentric cardiac hypertrophy and eccentric hypertrophy; in *Cardiac adaptations* (Springer) pp. 147–166
- Nakamura M and Sadoshima J 2018 Mechanisms of physiological and pathological cardiac hypertrophy. *Nat. Rev. Cardiol.* **15** 387–407
- Natarajan A, Yamagishi H, Ahmad F, *et al.* 2001 Human eHAND, but not dHAND, is down-regulated in cardiomyopathies. *J. Mol. Cell. Cardiol.* **33** 1607–1614
- Oktay AA, Aktürk HK, Paul TK, *et al.* 2020 Diabetes, cardiomyopathy, and heart failure; in *Endotext* (Eds) KR Feingold, B Anawalt, MR Blackman, *et al.* (South Dartmouth (MA): MDText.com, Inc.)
- Patel SK, Ramchand J, Crocitti V, *et al.* 2018 Kruppel-like factor 15 is critical for the development of left ventricular hypertrophy. *Int. J. Mol. Sci.* **19** 1303
- Quiñones MA, Otto CM, Stoddard M, *et al.* 2002 Recommendations for quantification of Doppler echocardiography: a report from the Doppler Quantification Task Force of the Nomenclature and Standards Committee of the American Society of Echocardiography. *J. Am. Soc. Echocardiogr.* **15** 167–184
- Rerych SK, Scholz PM, Sabiston DC Jr, *et al.* 1980 Effects of exercise training on left ventricular function in normal subjects: a longitudinal study by radionuclide angiography. *Am. J. Cardiol.* **45** 244–252
- Sayed D, Hong C, Chen IY, *et al.* 2007 MicroRNAs play an essential role in the development of cardiac hypertrophy. *Circ. Res.* **100** 416–424
- Soci UP, Fernandes T, Hashimoto NY, *et al.* 2011 MicroRNAs 29 are involved in the improvement of ventricular compliance promoted by aerobic exercise training in rats. *Physiol. Genomics* **43** 665–673
- Stansfield WE, Ranek M, Pendse A, *et al.* 2014 The pathophysiology of cardiac hypertrophy and heart failure; in *Cellular and molecular pathobiology of cardiovascular disease* (Elsevier) pp. 51–78
- Stein RA, Michielli D, Diamond J, *et al.* 1980 The cardiac response to exercise training: Echocardiographic analysis at rest and during exercise. *Am. J. Cardiol.* **46** 219–225
- Thattaliyath BD, Livi CB, Steinhilber ME, *et al.* 2002 HAND1 and HAND2 are expressed in the adult-rodent heart and are modulated during cardiac hypertrophy. *Biochem. Biophys. Res. Commun.* **297** 870–875
- Topkara VK and Mann DL 2010 Clinical applications of miRNAs in cardiac remodeling and heart failure. *Perspect. Med.* **7** 531–548
- Ucar A, Gupta SK, Fiedler J, *et al.* 2012 The miRNA-212/132 family regulates both cardiac hypertrophy and cardiomyocyte autophagy. *Nat. Commun.* **3** 1078

- van Rooij E and Olson EN 2009 Searching for miR-acles in cardiac fibrosis. *Circ. Res.* **104** 138–140
- van Rooij E, Marshall WS and Olson EN 2008a Toward microRNA-based therapeutics for heart disease: the sense in antisense. *Circ. Res.* **103** 919–928
- van Rooij E, Sutherland LB, Thatcher JE, et al. 2008b Dysregulation of microRNAs after myocardial infarction reveals a role of miR-29 in cardiac fibrosis. *Proc. Natl. Acad. Sci. USA* **105** 13027–13032
- Wang B, Haldar SM, Lu Y, et al. 2008 The Kruppel-like factor KLF15 inhibits connective tissue growth factor (Ctgf) expression in cardiac fibroblasts. *J. Mol. Cell. Cardiol.* **45** 193–197
- Wang L, Lv Y, Li G, et al. 2018 MicroRNAs in heart and circulation during physical exercise. *J. Sport Health Sci.* **7** 433–441
- Wang Y, Wisloff U and Kemi OJ 2010 Animal models in the study of exercise-induced cardiac hypertrophy. *Physiol. Res.* **59** 633
- Wijnen WJ, Pinto YM and Creemers EE 2013 The therapeutic potential of miRNAs in cardiac fibrosis: Where do we stand? *J. Cardiovasc. Transl. Res.* **6** 899–908
- Zheng Z, Zeng Y, Huang H, et al. 2013 MicroRNA-132 may play a role in coexistence of depression and cardiovascular disease: a hypothesis. *Med. Sci. Monit.* **19** 438

Corresponding editor: SREENIVAS CHAVALI